THE EFFECT OF INORGANIC COMPOSITES ON THE THERMAL DEGRADATION OF POLY(METHYL METHACRYLATE) (PMMA)

A THESIS SUBMITTED TO
THE GRADUATE SCHOOL OF NATURAL AND APPLIED SCIENCES
OF
MIDDLE EAST TECHNICAL UNIVERSITY

BY

MERYEM KARABULUT

IN PARTIAL FULFILLMENT OF THE REQUIREMENTS
FOR
THE DEGREE OF MASTER OF SCIENCE
IN
CHEMISTRY

SEPTEMBER 2011

Approval of the thesis:

THE EFFECT OF INORGANIC COMPOSITES ON THE THERMAL DEGRADATION OF POLY(METHYL METHACRYLATE) (PMMA)

submitted by **MERYEM KARABULUT** in partial fulfillment of the requirements for the degree of
Master of Science in Chemistry Department, Middle East Technical University by,

Prof. Dr. CANAN ÖZGEN _____
Dean, Graduate School of **Natural and Applied Sciences**

Prof. Dr. İlker ÖZKAN _____
Head of Department, **Chemistry**

Prof. Dr. Ceyhan KAYRAN _____
Supervisor, **Chemistry Dept., METU**

Prof. Dr. Jale HACALOĞLU _____
Co-supervisor, **Chemistry Dept., METU**

Examining Committee Members:

Prof. Dr. Nursel DİLSİZ
Chemical Engineering, GAZİ UNIVERSITY _____

Prof. Dr. Ceyhan KAYRAN
Chemistry Dept., METU _____

Prof. Dr. Jale HACALOĞLU
Chemistry Dept., METU _____

Assoc. Prof. Ayşen YILMAZ
Chemistry Dept., METU _____

Assist. Prof. İrem EREL
Chemistry Dept., METU _____

Date: _____

I hereby declare that all information in this document has been obtained and presented in accordance with academic rules and ethical conduct. I also declare that, as required by these rules and conduct, I have fully cited and referenced all material and results that are not original to this work.

Name, Last Name: MERYEM KARABULUT

Signature :

ABSTRACT

THE EFFECT OF INORGANIC COMPOSITES ON THE THERMAL DEGRADATION OF POLY(METHYL METHACRYLATE) (PMMA)

KARABULUT, Meryem

M.Sc., Department of Chemistry

Supervisor : Prof. Dr. Ceyhan KAYRAN

Co-Supervisor : Prof. Dr. Jale HACALOĞLU

September 2011, 53 pages

Metal coordinated polymer nanocomposites have gained great attention due to their superior characteristics. Polymethylmethacyrlate (PMMA) is the most commonly used polymer since it is easily processed. In this study, modified TiO_2 nanoparticles prepared by insitu and exsitu methods were embedded into PMMA in order to improve its thermal stability and the effects of TiO_2 nanoparticles on thermal characteristics of PMMA were investigated by direct pyrolysis mass spectrometry.

The insitu method which is a sol gel method, TiO_2 nanoparticles were synthesized by mixing titanium(IV) tetraisopropoxide, TTIP, with silane coupling agent, 3-(3-methoxysilyl)propylmethacrylate MSMA in absolute ethanol. In exsitu method, TiO_2 powder was directly mixed with silane coupling reagent. TiO_2/SiO_2 nanoparticles were embedded into the PMMA by direct mixing resulting in exsitu and insitu TiO_2/SiO_2/PMMA nanocomposites. The synthesized TiO_2/SiO_2/PMMA nanocomposites were characterized by TEM, ATR-FT-IR and analyzed for the investigation of their reaction mechanism and thermal characteristics by pyrolysis mass spectroscopy.

TEM images confirmed the formation of TiO_2/SiO_2 nanoparticles and TiO_2/SiO_2/PMMA nanocomposites and indicated that the average particle size of TiO_2/SiO_2 nanoparticles was around 6 nm whereas average particle size of SiO_2/TiO_2/PMMA nanocomposites were around 25 nm. The increase in the size of nanoparticles is associated with incorporation of TiO_2/SiO_2 nanoparticles into PMMA matrix.

ATR-FTIR spectrum of 5% TiO_2/SiO_2/PMMA nanocomposites showed the formation of TiO_2/SiO_2 nanoparticles clearly.

Pyrolysis mass spectrometry analysis revealed that incorporation of TiO_2/SiO_2 nanoparticles into PMMA resulted in higher thermal stability only for low weight percentage insitu TiO_2/SiO_2/PMMA. At high weight percentages a decrease in thermal stability was detected. On the other hand, in case of exsitu TiO_2/SiO_2/PMMA contrary to our expectations a decrease in thermal stability was detected. The decrease in thermal stability was attributed to evolution of methacrylic acid during thermal degradation of silane groups.

Keywords: PMMA, Polymer Nanocomposite, TiO_2, Sol Gel Method, Pyrolysis

ÖZ

İNORGANİK KOMPOZİTLERİN POLİMETİLMETAKRİLAT'IN ISIL DEGRADASYONU ÜZERİNDEKİ ETKİLERİ

KARABULUT, Meryem
Yüksek Lisans, Kimya Bölümü
Tez Yöneticisi : Prof. Dr. Ceyhan KAYRAN
Ortak Tez Yöneticisi : Prof. Dr. Jale HACALOĞLU

Eylül 2011, 53 sayfa

Metal bağlanmış nano yapılı polimer kompozitler üstün karakteristik özellikleri nedeniyle oldukça dikkat çekmektedir. Polimetilmetakrilat kolay işlenebilir olması nedeniyle en çok kullanılan polimerlerden biridir. Bu çalışmada, insitu ve exsitu methoduyla hazırlanan, modifiye edilmiş TiO_2 nano parçacıkları, PMMA'nın ısıl kararlılığını artırmak için içerisine gömülmüştür ve TiO_2 nano parçacıklarının PMMA'nın ısıl karakterine olan etkisi direk piroliz kütle spektrometrisiyle incelenmiştir.

Sol gel (insitu) metoduyla, TiO_2/SiO_2 nano parçacıkları, titanium (IV)tetraisopropoxide, TTIP ve silan bağlayıcı (3-(3-methoxysilyl)propylmethacrylate MSMA) etanol içerisinde karıştırılarak sentezlenmiştir. Exsitu metotda, toz halindeki TiO_2 direk olarak silan bağlayıcı ile karıştırılmıştır. TiO_2/SiO_2 nano parçacıkları, exsitu ve insitu TiO_2/SiO_2/PMMA nanokompozitleri oluşturacak şekilde, direk karıştırma yöntemiyle PMMA içerisine gömülmüştür. Sentezlenen TiO_2/SiO_2/PMMA nanokompozitler TEM, ATR-FT-IR spektroskopi teknikleri ile karakterize edilmiştir ve piroliz kütle spektroskopisi ile tepkime mekanizmaları ve ısıl karakterleri incelenmiştir.

TEM görüntüleri TiO_2/SiO_2 nano parçacıklarının ve TiO_2/SiO_2/PMMA nano

kompozitlerin oluşumunu doğrulamıştır. TiO_2/SiO_2/PMMA nano kompozitlerin ortalama parçacık boyutu 25 nm, TiO_2/SiO_2 nano parçacıklarının ortalama boyutu ise 6 nm olarak saptanmıştır. Nano parçacıklardaki boyut artışı, TiO_2/SiO_2 nano parçacıklarının PMMA içerisine katıldığını göstermektedir.

5% TiO_2/SiO_2/PMMA nano kompozitlerinin ATR-FT-IR spektrumu TiO_2/SiO_2 nano parçacıklarının oluşumunu açık bir şekilde göstermiştir.

Piroliz kütle spekrometri analizi, TiO_2/SiO_2 nano parçacıklarının PMMA içerisine katılmasının sadece düşük kütle yüzdeli insitu TiO_2/SiO_2/PMMA nano kompozitleri için ısıl kararlılıkta artış gösterdiğini açığa çıkarmıştır. Yüksek kütle yüzdeli olanlarda ısıl kararlılıkta azalma saptanmıştır. Öte yandan, exsitu TiO_2/SiO_2/PMMA durumunda beklenenin aksine,ısıl kararlılıkta azalma saptanmıştır. Isıl kararlılıktaki bu azalma, silan gruplarının ısıl bozulması sırasında metakrilik asit açığa çıkarmasına bağlanmıştır.

Anahtar Kelimeler: PMMA, Polimer Nanokompozit, TiO_2, Sol Gel Metod, Piroliz

To my husband

ACKNOWLEDGMENTS

The preparation of this important document would not have been possible without the support, hard work and endless efforts of a large number of individuals.

I would like to express my deep and sincere gratitude to my advisor Prof. Dr. Ceyhan Kayran. Her wide knowledge and her logical way of thinking have been of great value for me. Her understanding, encouraging and personal guidance have provided a good basis for the present thesis.

I am deeply grateful to my co-advisor Prof. Dr. Jale Hacaloğlu, for her detailed and constructive comments, and for her important support throughout this work.

I owe many many thanks to my lab partner, Tuğba Orhan who helped me to do the analysis of the research. She was always ready to give a hand whenever I needed. I truly thank to my dearest friends Rukan Koşak, Zafer Öztürk, Ebru Ünel and Berrin Özkan who were with me in this sometimes challenging process to share their valuable opinions and comments.

My deepest gratitude goes to my beloved parents who always supported me and believed in me.

Lastly, I am forever grateful to my husband for his patience, support and belief in me. It makes me feel an extraordinarily lucky person to know that he was, is and will be there for me whenever I call for help.

TABLE OF CONTENTS

LIST OF TABLES

TABLES

LIST OF FIGURES

FIGURES

LIST OF SCHEMES

SCHEMES

CHAPTER 1

INTRODUCTION

1.1 Nanomaterials

Over the past decades, nanomaterials have become one of the most popular research areas for the scientists since they have superior advantages. Nanomaterials can be any material such as metals, ceramics, polymeric materials, or composite materials. Nanomaterials have many applications which are currently in use in areas such as medicine, food, clothing, defense, national security, environmental clean-up, energy generation, electronics, computing and construction [1].

Nanotechnology is a wide area which includes polymer science and technology as a promising branch, and polymer science and technology covers lots of other areas in it. Polymer matrix based nanocomposites have gained great attention since they give the characteristics of two different worlds of chemistry. Hybrid materials which are the combination of organic and inorganic materials get attention in nanotechnology as the best characteristics of each component can be intercooperated. The word nanocomposite is used for materials that consist at least one phase having one dimension less than 100 nm. Organic/inorganic nanocomposites are polymer composites which have inorganic nanoscale building blocks. While engineering a polymer nanocomposite it is important to keep the advantages and to isolate the disadvantages of the materials individually.

Small size of the inorganic component is the major reason of improved properties of polymers. Polymer nanocomposites have different properties than bulk polymer since inorganic nanoparticles increase the interfacial area with the polymer [2].

Nanocomposite materials can be classified in three cathegories ;

- Ceramic matrix nanocomposites (CMNC)
- Metal matrix nanocomposites (MMNC)
- Polymer matrix nanocomposites (PMNC)

Polymer matrix nanocomposites are the main focus of this study. As the name implies polymer matrix nanocomposites are the materials that have the polymers as the host material. Polymer nanocomposites are defined as systems having two phases; one of which is high surface area fillers. In this concept, in theory, every single property of the polymer such as mechanical, optical and thermal properties can be improved by the help of the fillers, even at low loadings [3]. Inorganic parts of the composites, which are called fillers, have superior characteristics over polymers such as rigidity and thermal stability whereas organic polymers are flexibile, dielectric, ductile and processable.

Hybrid term is used when two moieties are combined at the molecular level one of which is organic and the other inorganic in most cases. The nanocomposite term is used if one of the moiety is at the nano scale. In the case where the inorganic part of the hybrid is prepared by sol gel method composites having dimensions less than 100 nm can be produced.

Combination of these two important kinds of materials gave us a chance to create a new material with new properties. Inorganic nanoscale compartments of the hybrids can be nanotubes, layered silicates, nanoparticles of metals, oxides of metals or semiconductors [4].

Among these materials, metal oxides are important fillers. Incorporation of metal oxide nanoparticles into the polymer matrix has attracted great attention [5–10]. Many studies were done to investigate the effect of metal oxide nanoparticles on polymers such as thermal stability, catalytic activity, optical behaviour, flame retardancy.

While preparing a polymer nanocomposite it is very important to follow logical steps and choose proper materials depending on which product is desired. First of all, for

the polymeric part a precursor can be chosen, such as a monomer or oligomer. A polymer network or linear polymers, which can be molten or solution, can also be used. The same thing can be applied to inorganic part either using the precursor or the prepared nanoparticle of metals as the starting material [11].

There are several preparation methods such as, interclation of nanoparticles with the polymers or pre-polymer solution, in-situ intercalative polymerization, melt intercalation, direct mixture of polymer and inorganic particulates, template synthesis, in-situ polmerization, and sol gel process [12].

1.2 Preparation Methods for Nanocomposites

There are three main categories of mixing nanoparticles into the polymer. These are direct mixing or blending, sol gel process and in-situ polymerization.

1.2.1 Direct Mixing Method

In general, in direct mixing method nano particles and the polymer sample with different weight percentages are mixed through either a melt mixing or solution mixing process. Each mixture was reinjected several times to get a uniform dispersion. Several examples for application of direct mixing in which TiO_2 was used as nanoparticles appeared in the literature [13-14].

Chatterjee et. al. synthesized a nanocomposite by directly mixing nano TiO_2 and PMMA observed increase in its stability [15]. Rong et. al. prepared nanocomposites by using polystyrene and TiO_2 nanoparticles [16]. TiO_2 nanoparticles were used either as received, dried or modified with silane coupling agent. All of the nanoparticles were mixed with the polymer at high temperatures. The initial decomposition temperature of polystyrene was 275 °C whereas SiO_2/TiO_2/PS increased to 347 °C. Laachi et.al. synthesized PMMA/ZnO nancomposites by direct mixing of polymer and nano ZnO particles [17]. They prepared molten PMMA pellets and mixed them with the fillers using twin-screw extruder. The thermal characterization of the PMMA/ZnO nanocomposites showed that the thermal

degradation stability of PMMA/ZnO nanocomposites increased compared to pure PMMA. Decomposition temperature of neat PMMA increased from 312 to 348 °C.

The main problem in nanocomposites, prepared by direct mixing, is the weak interactions, hydrogen bonds and van der Waal forces, between the polymer and the inorganic part. Another problem is the agglomeration of nanoparticles. These problems make the method non-preferential.

1.2.2 Sol Gel Method

Sol gel is a common method which was developed by Geffcen and Berger in 1930. Since then, this process was applied to many metal species. Sakka, a pioneer in this area, believes that sol gel is a branch of nanotechnology since the products of this process contain nanoparticles in it [18].

Sol gel process is a useful way of making new and advanced materials in which different forms of materials can be produced by changing the synthesis route. This method is a waste free method and is ecologically friendly. Sol gel method can be defined in a simple way as a process going from solution to gel state to form different kinds of materials such as ceramic fibers, aerogels, xerogels, dense ceramics and dense films [19].

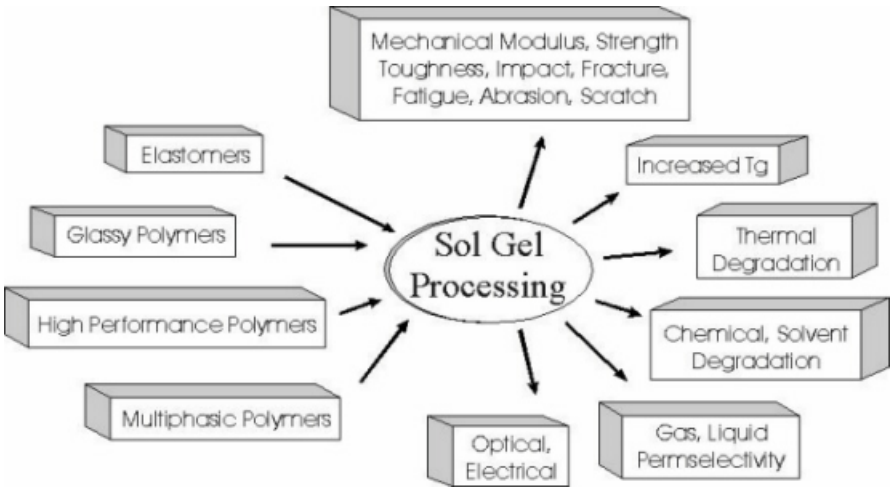

Figure 1.1: Sol gel processing

Sythesis of high purity metal oxides can be achieved by the hydrolysis of alkoxides

of metals to produce OH attached metals. Then, condensation reactions follow to produce metal oxides. At the end of these series of reactions removal of solvent is the last step. As it is seen from the mechanism given in Scheme 1.1 sol gel technology is a very useful and easy method for the synthesis of metal oxide nanoparticles [20–29].

Scheme 1.1: General representation of sol gel

$$M(OR)_4 + 4H_2O \longrightarrow M(OH)_4 + 4ROH,$$
$$mM(OH)_4 \longrightarrow (MO_2)_m + 2mH_2O.$$

Yuwono et. al. was able to synthesize TiO_2 nanoparticles by sol gel method. They used titanium (IV) tetraisopropoxide (TTIP) as the precursor of TiO_2 [30]. They dissolved TTIP in alcohol and added silane coupling agent to make it compatible with the polymer. Then, they mixed the modified TiO_2 nanoparticles with the polymer by solution mixing to produce a polymer nanocomposite. Zheng et. al. synthesized SiO_2/PMMA nanocomposites with weight percentages of 1%, 2%, 3% of SiO_2 via insitu polymerization method. An enhanced thermal stability of SiO_2/PMMA with 1% of SiO_2 content is observed by TGA [31].

Haitao Wang et. al. prepared polyimide/silica composites via sol gel method [32].They started with the water glass as silicic acid precursor. The synthetic route was from silicic acid to silicic acid oligomer and finally to silica network. They found that the decomposition temperature of the hybrid composites are higher than the pure polyimide (PI); thermal decomposition temperature of PI increased from 551 to 566 °C with addition of 20% silica content.

1.2.3 In Situ Polymerization Method

Polymer nanocomposites can be achieved by the polymerization of monomer in the presence of metal nanoparticle.

In insitu polymerization method the interaction between the organic and inorganic phases increases while agglomeration decreases. But, still, it is difficult to remove

unreacted materials, and to control the reaction conditions, requiring high purification techniques.

To generalize, it is true to say that there is more than one way to synthesize polymer/metal oxide nanocomposites. Combinations of two or more procedures can be applied to materials according to what is aimed to produce.

1.3 Poly(methyl methacrylate), (PMMA) / TiO_2 Nanocomposites

1.3.1 PMMA

Polymethylmethacrylate is a member of thermoplastic polymer group. It has great advantages such as, excellent clarity and UV shielding properties. In addition to these, it has good abrasion resistance, hardness and stiffness. Also, it has low water absorption and low smoke emission.

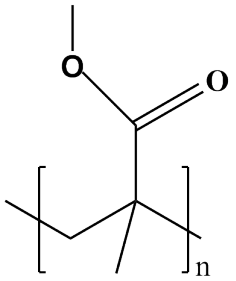

Figure 1.2: Open Structure of Poly(methyl methacrylate)

PMMA is a versatile polymer and has a wide variety of application areas since it is easily processed and is a low cost polymer [33].

In order to improve thermal stability and thermal degradation characteristics of PMMA various methods are used. Among these addition of TiO_2 and modified TiO_2 nanoparticles have gained significant interest.

1.3.2 TiO_2

TiO_2 is a white pigment which has ability to scatter UV light. It gives whiteness, brightness, and high opacity when embedded into polymers. TiO_2 crystals exist in three different forms, namely; rutile, anatase and brookite. Among these forms, rutile is the most stable one. However, anatase receives great attention due to its high catalytic activity and wide application areas in the industry.

As mentioned earlier, TiO_2 is an attractive candidate as a favorable metal oxide owing to its important characteristics such as;

- Strong oxidizing agent at moderate temperature and pressure
- Antibacterial
- Self-cleaning
- Depolluting
- Chemically inert
- Physically stable
- Non-toxic
- Superhydrophilic
- Cheap and readily available

By taking TiO_2's important characteristics into consideration, this metal oxide has been widely employed in the industry. To illustrate, it has been used in Japan as a coating material for buildings and highway barriers with the aim of NOx reduction and self cleaning. Moreover, TiO_2 is being used for the production of photocatalitically active materials in Europe.

Also, some studies were dedicated to test the efficiency of TiO_2 in the degradation of NOx and VOC gas in America.

In addition to these application areas, TiO_2 can also be used in order to improve the thermal stability of the polymers by the incorporation of this metal oxide into polymer

matrices owing to the high thermal stability and surface area of TiO_2 as a catalyst which provides higher thermal stability to the incorporated polymer [34]

1.3.2.1 Synthesis of TiO_2 Nanoparticles

Synthesis of TiO_2 Nanoparticles via Sol Gel Method: Sol-gel method is widely applied in order to prepare TiO_2 nanoparticles. Basically, sol-gel method is the hydrolysis which is followed by the stepwise condensation reactions of an alkoxide or halide precursor of the metal and to form inorganic networks [35–45]. In an aqueous medium, the general reaction mechanism is given below in Scheme 1.2.

Scheme 1.2: Reaction scheme of sol-gel process in aqueous medium.

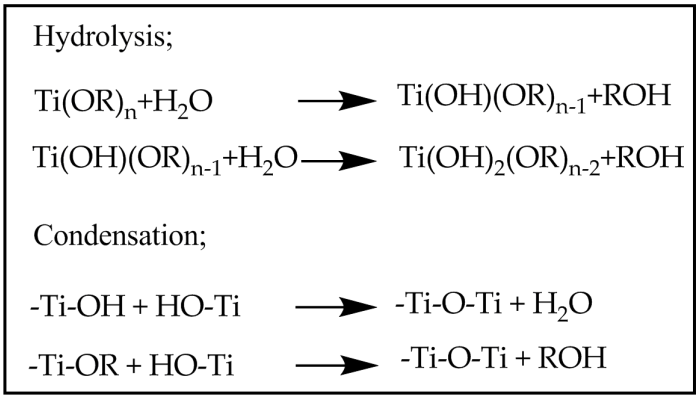

The reactions can be carried out in an alcoholic medium as an alternative as shown in Scheme 1.3.

Scheme 1.3: Reaction scheme of sol-gel process in alcoholic medium.

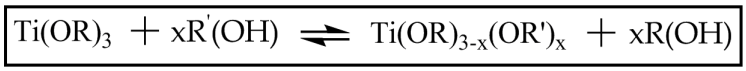

However, alcoxolation, oxolation, and olation reactions (Scheme 1.4) compete with the essential reactions; hydrolysis and condensation. These reactions are;

Scheme 1.4: General representation of a) Alcoxolation b) Oxolation c)) Olation reactions.

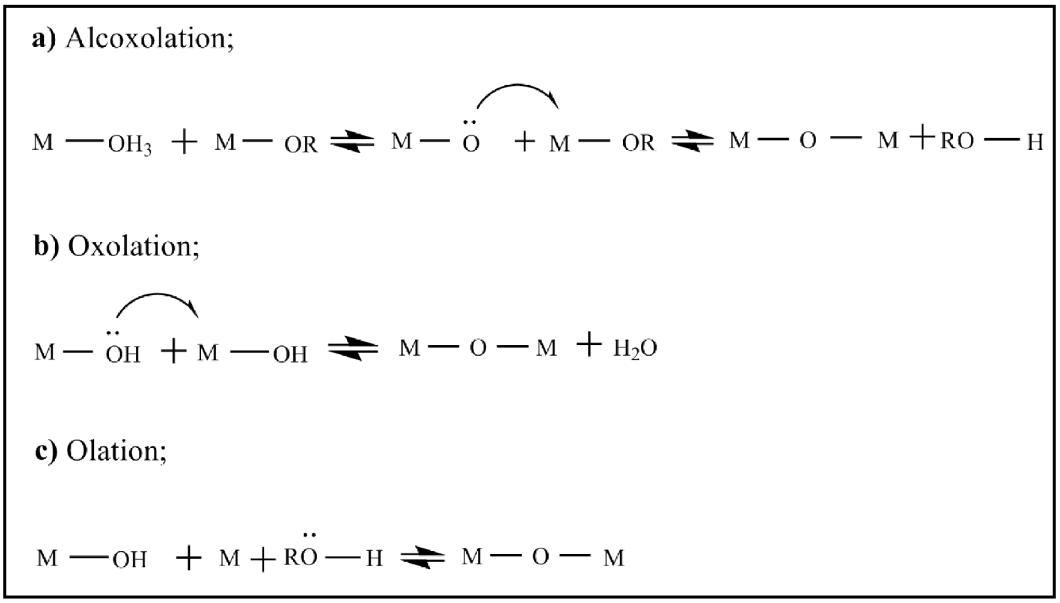

The amount of water used is the crucial point in the synthesis of titanium dioxide nanoparticles. Owing to the fact that water increases the rate of hydrolysis, the formed Ti-O-Ti networks will be packed loosely in the presence of excess water. On the contrary, low amount of water favors the aloxolation reactions to produce tightly packed and three dimensional networks [4].

Synthesis of TiO_2 Nanoparticles via Micelles or Inverse Micelles: Micelles or inverse micelles are being utilized in order to control the size and the shape of the prepared TiO_2 nanoparticles. Micelles have two functional ends, hydrophobic and hydrophilic. Hydrophobic hydrocarbon chains are towards inside the micelle whereas hydrophilic ends form a surrounding with the aqueous medium. In the same sense, reverse micelles are the ones which have hydrophobic ends towards nonaqueous medium.

Synthesis of TiO_2 Nanoparticles via Hydrothermal Method: Hydrothermal method is widely used in ceramic industry for the production of very small powders and productions are carried out in the autoclaves at suitable pressures and temperatures.

Synthesis of TiO_2 Nanoparticles via Solvothermal Method: Solvothermal method is the combination of non-hydrolytical sol-gel and hydrothermal method in the sense that it requires use of nonaqueous solvent and high temperatures. Therefore, this

method takes advantages of both methods such as size and shape control and high crystallinity.

Synthesis of TiO_2 Nanoparticles via Chemical Vapor Deposition Method: In this process, metal oxide precursor is exposed to one or more volatile precursor which reacts with the substrate so as to produce desired material.

1.3.2.2 Modification of TiO_2

Nanoparticles have become essential components for the industrial purposes due to their superior chemical and physical properties. Because of their diverse surface properties, nanoparticles have different interactions which may result in aggregation and dispersion problems. Hence, it has become a very important issue to modify the nanoparticles so that these problems can be overcome. Surface modification is one of the most favorable methods used for increasing dispersibility and preventing aggregation of the nanoparticles in the medium [46–52].

Silane coupling agents have the desirable properties. They form a bond between inorganic and organic materials. They have become an important tool for the area of chemistry in which surfaces have been modified in order to generate environments that are turned into uniform composites from different phases [53, 54]. General form of silane coupling agents is shown below in Figure 1.3.

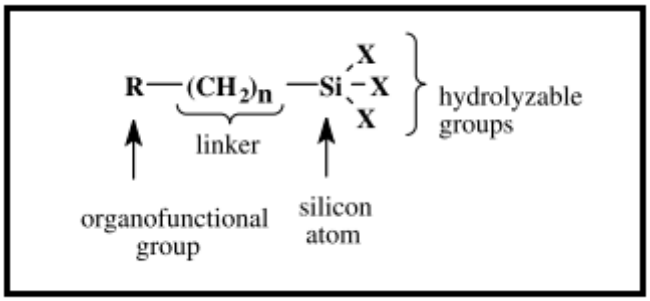

Figure 1.3: General formula of silane coupling agents

Reactions between metal oxides and silane coupling agents result in a complex which has high stability and functionality. 3-(trimethoxysilyl)propyl methacrylate (MSMA)

is a silane coupling agent which has two functional ends as shown in Figure 1.4. Alkoxide ends react with the OH groups that are attached to the surface of the TiO_2 to form Ti-O-Si bonds. As a result, modified TiO_2 has a highly stable network structure and attached vinyl end group makes this complex compatible with the polymer [55].

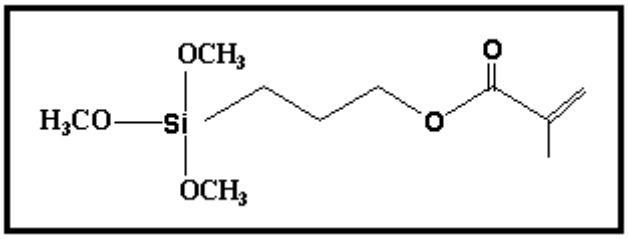

Figure 1.4: Open formula of 3-(trimethoxysilyl) propylmethacrylate (MSMA)

In insitu method, silane coupling agent is added to TiO_2 nanoparticles during the synthesis process of TiO_2. Some of the alkoxide groups present in titania precursor and silane coupling agent are hydrolyzed under the experimental conditions as shown in Scheme 1.5. Then, the reactions between alkoxide ends and OH groups yield modified TiO_2 as shown in Scheme 1.6.

Scheme 1.5: Hydrolysis of titanium(IV) tetraisopropoxide (TTIP) and 3-(3-methoxysilyl)propylmethacrylate (MSMA) in acidic medium

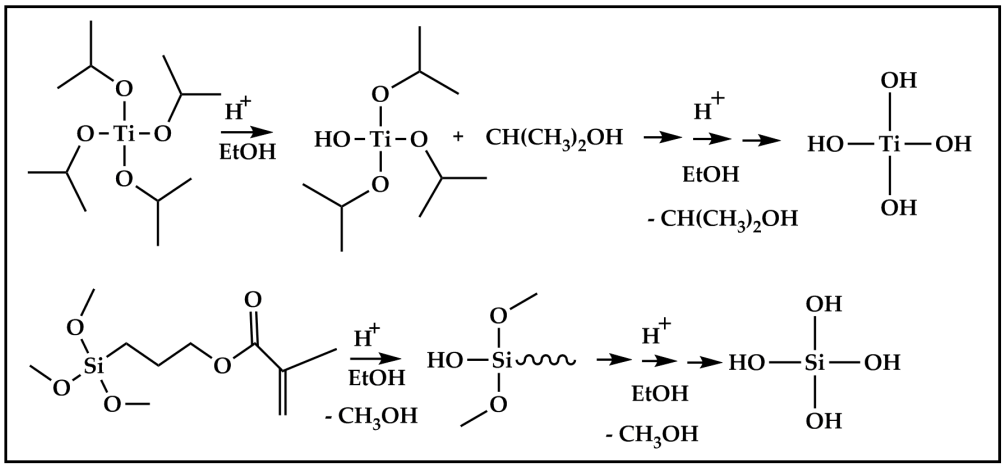

In case of exsitu method, silane coupling agent is added directly to TiO_2 powder (Scheme I.7).

Scheme 1.6: Insitu modification of titania between titanium(IV) tetraisopropoxide and silane coupling agent to form insitu TiO_2/SiO_2 functionalized metal

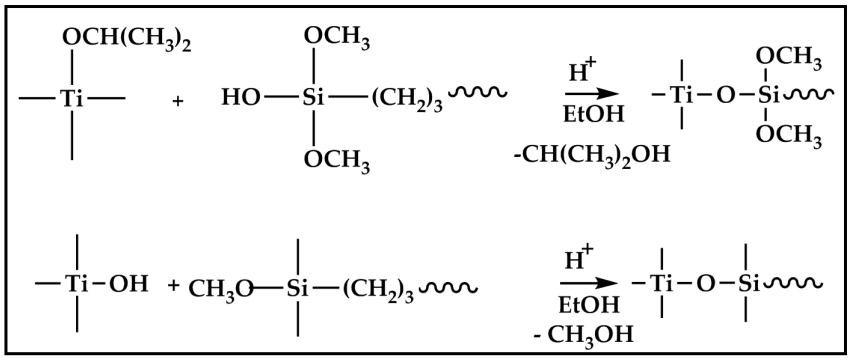

Scheme 1.7: Exsitu modification of titania powder with silane coupling agent to form TiO_2/SiO_2 functionalized metal

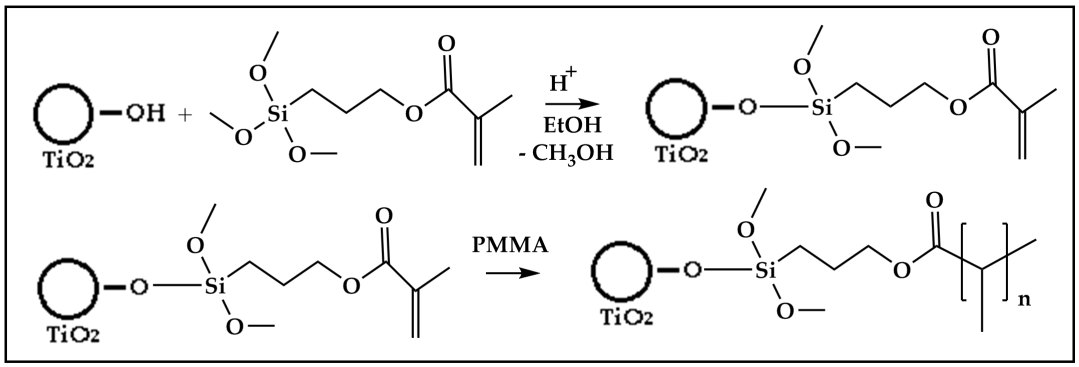

1.3.3 TiO_2/PMMA Composites

Viratyaporn et. al. synthesized Al_2O_3/PMMA and ZnO/PMMA nanocomposites via insitu bulk polymerization. Increase in thermal stability of PMMA and change in thermal degradation mechanism of PMMA was observed upon addition of nanoparticles. The reason of improvement of thermal stability was attributed to decrease in polymer chain mobility and elimination of free radical by the addition of nanoparticles [56]. Laachachi et. al. synthesized PMMA/TiO_2 by incorporation of TiO_2 and modified TiO_2 with organoclays and determined the thermal and flammability properties of PMMA [57, 58].

Caris et. al. incorporated TiO_2 into PMMA by emulsion polymerization [59]. Sidorenko et. al. initiated the radical polymerization of styrene

and methyl methacrylate (MMA) at the surface of TiO_2 particles to prepare PS/TiO_2 and PMMA/TiO_2 nanocomposites respectively [60]. Erdem et. al. prepared PS/TiO_2 nanocomposites by miniemulsion polymerization [61]. Rong et. al. synthesized PMMA/TiO_2 by using TiO_2 nanoparticles modified by 3-(trimethoxysilyl)propylmethacrylate (MPS), and styrene monomer [16].

Mingjiao Yang and Yi Dan have prepared TiO_2/PMMA composite partical via in-situ emulsion polymerization [62]. DTG curve of pure PMMA shows two overlapped peaks (about 300 and 340 °C). Incorporation of TiO_2 nanoparticles shiftted decomposition to higher temperature for TiO_2/PMMA; only one peak at 372 °C. Zhang et. al. synthesized TiO_2/polypyrole composite by emulsion polymerization [63]. Koziej et. al. have prepared insitu and exsitu TiO_2/PMMA by direct mixing method [64]. TGA measurements of both insitu and exsitu TiO_2/SiO_2 nanoparticles showed that insitu synthesized TiO_2/SiO_2 has higher thermal stability.

Chatterjee et. al. synthesized a nanocomposite by directly mixing nano TiO_2 and PMMA through a melt mixing process with different weight percentages [15]. Twin screw extruder was set to a temperature higher than melting point of PMMA. The thermal stability of the nanocomposites increased about 50 °C with nano TiO_2 addition.

Dzunuzovic et. al. used sol gel method to synthesize TiO_2 and insitu polymerization to synthesize PMMA [65]. They started with titanium tetrachloride as precursor of titania, silicic acid as the precursor of silane and dissolved it in alcohol and dried the product to produce TiO_2/SiO_2 nanoparticles. Then, these nanoparticles were mixed with MMA monomer to produce TiO_2/SiO_2/PMMA nanocomposites. TGA results showed that the thermal stabilities of the PMMA polymer can be improved by the addition of nanometer-scale silica/titania inorganic particles. Thermal decomposition temperature of PMMA increased about 40 °C upon addition of 20% TiO_2/SiO_2 nanoparticles.

Though several studies on preparation and applications of TiO_2/SiO_2/PMMA have been carried out, the knowledge of reaction mechanism and thermal characteristics that are very important for investigation of synthesis routes and application areas is limited. Among several thermal analysis methods, pyrolysis mass spectrometry

(py-MS) is one of the methods that give information on not only thermal stability but also on thermal degradation products.

In this study, our aim is preparation and structural and thermal characterization of TiO_2/SiO_2/PMMA nanoparticles. The modified TiO_2 nanoparticles were prepared by both exsitu method in which TiO_2 powder was modified with silane coupling agent 3-(3-methoxysilyl) propylmethacrylate, (MSMA), and insitu method, in which titanium(IV) tetraisopropoxide, TTIP, was modified again with silane coupling agent, (MSMA). Structural characterization of samples was achieved by application of TEM and ATR-FTIR methods and the effects of modification method and the weight percentage of TiO_2/SiO_2 nanoparticles on thermal characteristics of PMMA were investigated by direct pyrolysis mass spectrometry.

CHAPTER 2

EXPERIMENTAL

2.1 Chemicals

The transition metal oxide, TiO_2 and the precursor for the TiO_2, titanium(IV) tetraisopropoxide, TTIP were purchased from Merck and Acros Organics respectively. 3-(3-methoxysilyl) propylmethacrylate (MSMA) used as coupling agent or modifying agent was purchased from Across Organics. Polymethylmethacrylate, PMMA was also purchased from Across Organics. Toluene purchased from Sigma Aldrich was used after purification by refluxing over metallic sodium under nitrogen for two or three days. Absolute ethanol from J.T. Baker was used as received.

2.2 Synthesis and Insitu Modification of TiO_2

4.31 mL of titanium(IV) tetraisopropoxide, TTIP was added to 8.74 mL of absolute ethanol yielding 1:10 (TTIP/ethanol) molar ratio. Then 0.2 mL of 3-(3-methoxysilyl) propylmethacrylate, MSMA with a 0.06:1 molar ratio (MSMS/TTIP) and 0.4 mLof 0.05 M HCl was added to this mixture (Scheme 1.5) and stirred under vigorous stirring for 3 hours. Resultant cloudy and opaque solution was poured into a petri dish and dried at 80°C in vacuum. The dried product was purified with soxhlet apparatus to remove unreacted MSMA for 72 hours (Table 2.1). Soxhlet apparatus was shown in Figure 2.1. The remained solid product was used characterized by TEM, FT-IR and direct pyrolysis mass spectrometry.

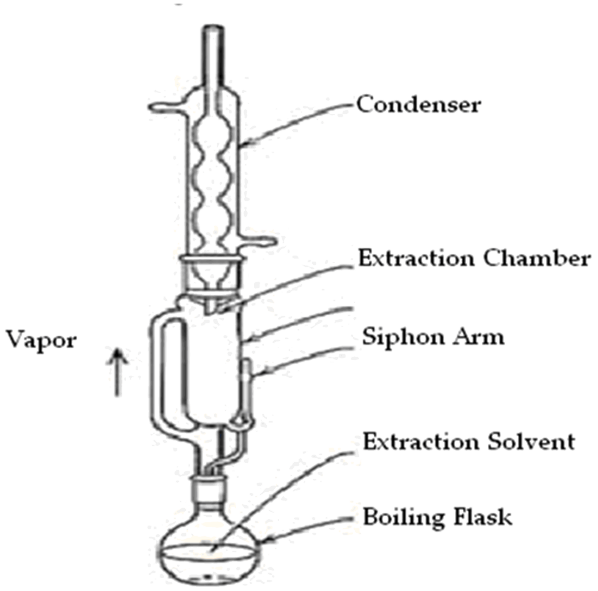

Figure 2.1: The Soxhlet Apparatus Used For The Purification

2.3 Exsitu Modification of TiO_2

100 mg of TiO_2 powder was dissolved in 20 mL of ethanol. 0.6 mL of silane coupling agent, MSMA, was added to the reaction medium. The reaction is shown in Scheme 1.7. The mixture was stirred for 4 hours until a uniform solution was observed. The product was purified with a soxhlet apparatus to remove MSMA adsorbed on the surface of TiO_2 to have pure exsitu TiO_2/ SiO_2.

Table 2.1: The reactants used to form insitu and exsitu functionalized titania.

Coupling Agent	Metal precursor	Product
3(trimethoxysilyl) propylmethacrylate MSMA	Titanium(IV) tetraisopropoxide (TTIP)	Insitu TiO_2/SiO_2
	TiO_2 powder	Exsitu TiO_2/SiO_2

2.4 Preparation of PMMA/TiO_2 Nanocomposite

100 mg of PMMA was dissolved in 15 mL of toluene by stirring overnight. TiO_2/SiO_2 nanoparticles which were prepared acccording to insitu or exsitu methods (Schemes 1.5, 1.6 and 1.7) were introduced by different weight percentages into the solution containing PMMA. The final mixture was stirred for about 4 hours. Finally, the solvent was evaporated under vacuum. The products (Table 2.2) were characterized by means of TEM, ATR-FTIR and direct pyrolysis mass spectrometry techniques.

Table 2.2: Prepared PMMA nanocomposites

Polymer	**TiO_2 precursor**	**Silane coupling agent**	**Metal**	**Polymer Nanocomposite**
PMMA	titanium(IV) tetraisopropoxide TTIP	3-(3-methoxysilyl) propylmethacrylate MSMA	Insitu TiO_2/SiO_2	Insitu TiO_2/SiO_2/PMMA
	TiO_2		Exsitu TiO_2/SiO_2	Exsitu TiO_2/SiO_2/PMMA

2.5 Characterization

2.5.1 Transmission Electron Microscopy TEM

Transmission electron microscopy (TEM) imaging of the nanoparticles was carried out with a FEI Tecnai G2 F30 instrument at 120 kV. The nanoparticles were dispersed on the carbon coated grid from their diluted suspension in toluene. The synthesis of the metal nanoparticles were confirmed by TEM.

2.5.2 ATR-FT-IR Spectra

ATR-FT-IR analyses of the samples were performed by directly insertion of solid samples using Bruker Vertex 70 Spectrophotometer.

2.5.3 Direct Pyrolysis Mass Spectrometry

DP-MS analysis were made by using Waters Micromass Quattro Micro GC Mass Spectrometer with a mass range from 10 to 2000 Da and EI ion source coupled to a direct insertion probe. During the pyrolysis, the temperature was increased to 50°C at a rate of 5 °C/min., then was raised to 650 °C with a rate of 10 °C/min. and kept at 650 °C for 5 minutes with recording 70 eV EI mass spectra at a mass scan rate of 1 scan/s. Deep capillary quartz tubes were used as sample container.

CHAPTER 3

RESULTS AND DISCUSSION

The characterization of the polymer nanocomposites were done by the transmission electron microscopy (TEM), FTIR and direct pyrolysis mass spectrometry techniques.

3.1 Transmission Electron Microscopy (TEM) Analysis

The TEM images of SiO_2/TiO_2 nanoparticles and %10 insitu, %10 exsitu, %30 insitu SiO_2/TiO_2/PMMA nanocomposites are shown in Figure 3.1., Figure 3.2., Figure 3.3. and Figure 3.4. respectively. Average particle size of SiO_2/TiO_2 nanoparticles is around 6 nm whereas average particle size ofSiO_2/TiO_2/PMMA tertiary nanocomposites are around 25 nm. Increase in the size of nanoparticles is due to incorporation of SiO_2/TiO_2 nanoparticles into PMMA matrix.

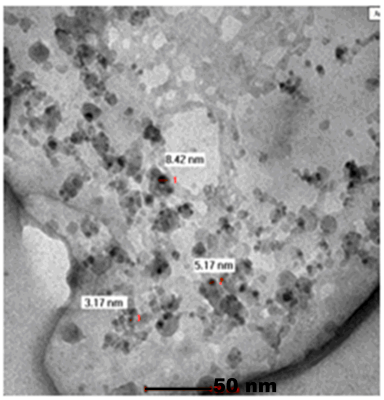

Figure 3.1: TEM images of SiO_2/TiO_2 nanoparticles

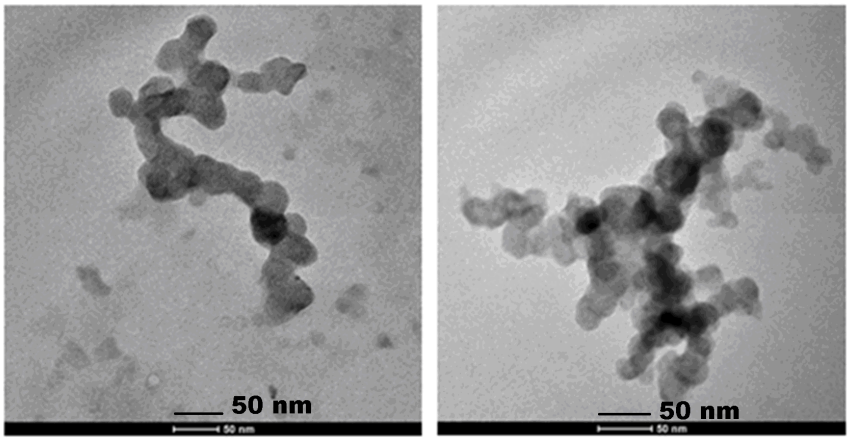

Figure 3.2: TEM images of %10 insitu TiO_2/SiO_2/PMMA nanoparticles

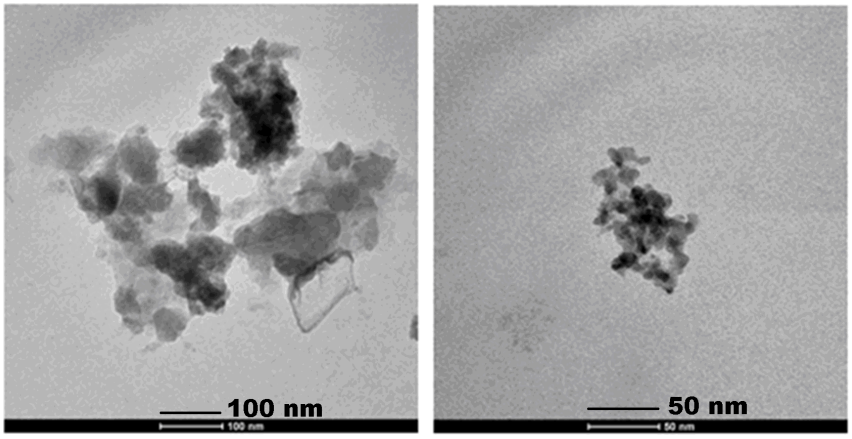

Figure 3.3: TEM images of %10 exsitu TiO_2/SiO_2/PMMA nanoparticles

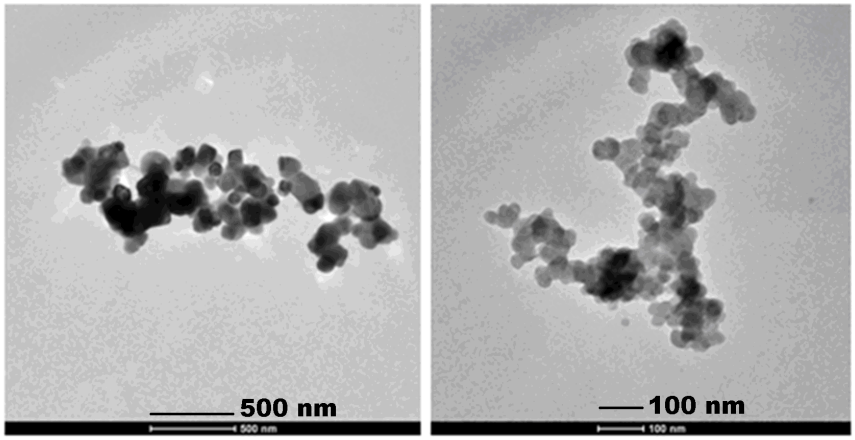

Figure 3.4: TEM images of %30 insitu TiO_2/SiO_2/PMMA nanoparticles

3.2 ATR-FT-IR Characterization

The characteristic absorption bands corresponds to the vibrations of v(C-H) belonging to silane coupling agent (MSMA) normally comes at around 2300-2500 cm^{-1}, v(Si-O-CH3) at 1200-1400 cm^{-1}, and v(Si-O-Ti) at 930 cm^{-1}, v(Si-O-Si) at 800-820 cm^{-1}. Ti-O-Ti stretching was expected to appear around 400 cm^{-1} [13]. The prominent bands belonging to PMMA are the C=O stretch coming at 1730 cm^{-1}, the asymmetric C-C-O stretch at 1270 and 1240 cm^{-1}, the asymmetric C-O-C stretch 1190 and 1150 cm^{-1} and the C-C skeletal stretch at around 750 cm^{-1} (Table 3.1) [66].

Table 3.1: The characteristic IR stretching frequencies related with TiO_2/SiO_2/ PMMA

Bond	**IR Stretching Frequency Range, cm^{-1}**
Si-O-Si	600-850
Ti-O-Si	900-1000
Si-O-CH_3	1250-1400
H_2O (on the surface of nano TiO_2)	1600
Ti-O-Ti	400
C-H (in MSMA)	2300-2500
C=O (in PMMA)	1730
the asymmetric C-C-O stretch	1270 and 1240
the asymmetric C-O-C stretch	1190 and 1150
the C-C skeletal stretch	750

ATR-FT-IR spectra of insitu and exsitu TiO_2/SiO_2/PMMA were evaluated using 5% w/w incorporated TiO_2/SiO_2 into PMMA (Figure 3.1). Ti-O-Ti and Si-O-Si stretching peaks appeared clearly at around 400 cm^{-1} and 700 cm^{-1} in the ATR-FT-IR spectra respectively. In addition to this, a new absorption peak showed up at around 925 cm^{-1} indicating Ti-O-Si bond formation. This would be nice evidence that TiO_2/SiO_2 network formed properly so that it could be incorporated into PMMA as planned. The characteristic absorption peak of the carbonyl group of PMMA appeared at around 1730 cm^{-1} and did not change after TiO_2/SiO_2/PMMA formation. This indicated that

covalent bond formed between PMMA and silane coupling agent occurs from vinyl end of silane coupling agent MSMA.

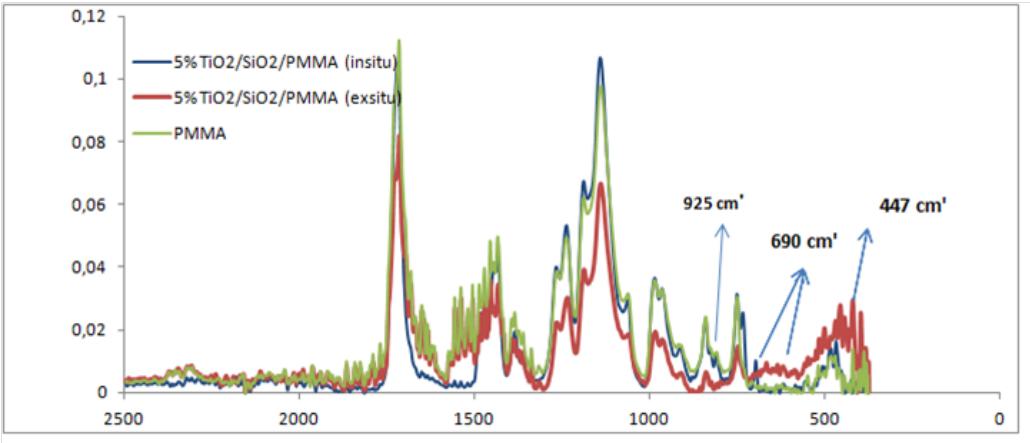

Figure 3.5: The FT-IR spectra of %5 (w/w) incorporation of TiO_2/SiO_2 into PMMA

Thus, TEM and ATR-FT-IR spectroscopy results confirmed formation of TiO_2/SiO_2/PMMA nanoparticles.

3.3 Thermal Characterization of TiO_2/SiO_2 functional PMMA

Thermal degradation behavior of poly(methylmethacrylate), and TiO_2/SiO_2 functional PMMA, namely exsitu and insitu TiO_2/SiO_2/PMMA were studied via DP-MS technique. Exsitu TiO_2/SiO_2/PMMA was prepared using TiO_2 powder modified with silane coupling agent, 3-(3-methoxysilyl) propylmetacrylate, (MSMA), whereas, insitu TiO_2/SiO_2/PMMA was prepared using titanium(IV) tetraisopropoxide, TTIP, modified with silane coupling agent, (MSMA).

3.3.1 Poly(methylmethacrylate)

It is known that poly(methylmethacrylate), (PMMA), degrades via a mixture of chain end and random chain scission initiation followed by depropagation which produces mostly monomer and low molecular weight oligomers as shown in Scheme 3.1. [67, 68].

Scheme 3.1: Thermal degradation mechanism of poly(methyl methacrylate)

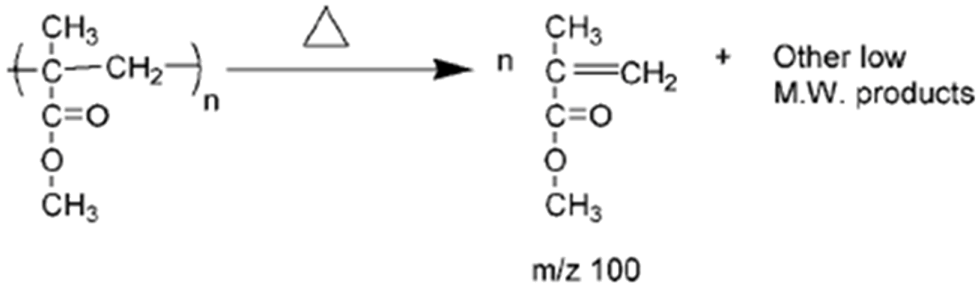

Total ion current, (variation of total ion yield as a function of temperature/time), (TIC) curve and the pyrolysis mass spectra at the maximum of the peaks present in the TIC curve at 324 and 424 °C recorded during the pyrolysis of PMMA are shown in Figure 3.6.

The pyrolysis mass spectra at these temperatures show classical fragmentation pattern of the monomer, methyl methacrylate, confirming depolymerization [69].

Single ion evolution profiles (variation of ion yield as a function of temperature) of intense and/or characteristic products, namely monomer (m/z=100 Da), $CH_2C(CH_3)CO$ (m/z=69 Da) and CH_2CCH_3 (m/z=41 Da) are given in Figure 3.7. The yields of the products of PMMA were maximized at around 324 and 424 °C. The low temperature peak can be attributed to presence of low molar mass chains.

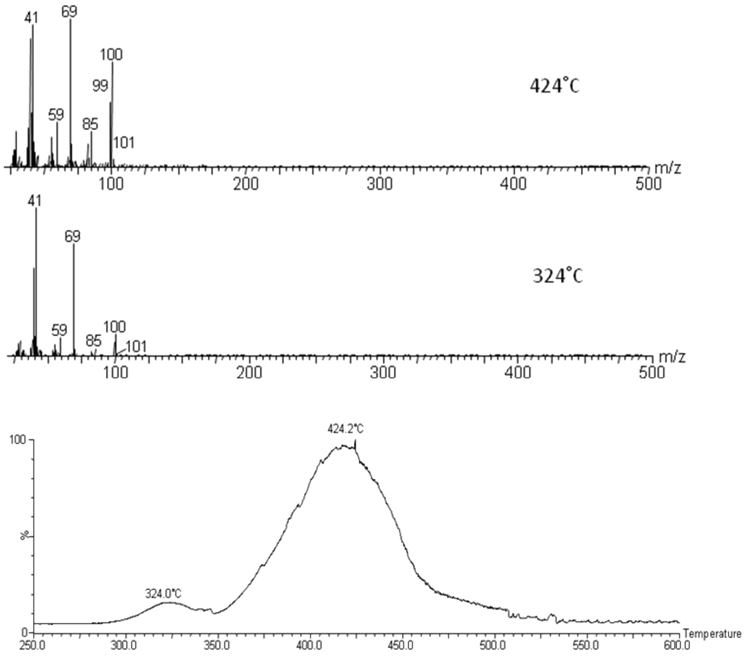

Figure 3.6: The TIC curve and the pyrolysis mass spectra recorded during the pyrolysis of PMMA.

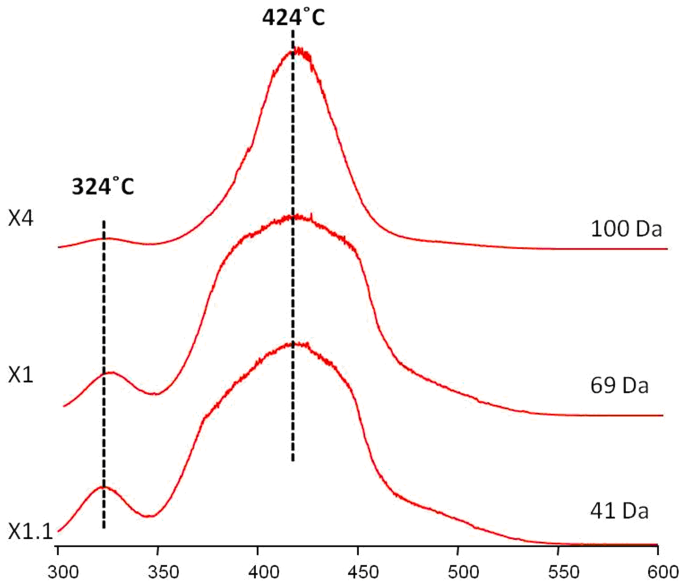

Figure 3.7: Single ion evolution profiles of some selected thermal decomposition products of PMMA

3.3.2 TiO_2/SiO_2

In this study, TiO_2/SiO_2 was used as the metal oxide source. So, thermal behaviors of the TiO_2/SiO_2 nanoparticles were also investigated. Thermal degradation characteristics of TiO_2 powder modified with silane coupling agent, 3-(3-methoxysilyl) propylmethacrylate, (MSMA), and titanium(IV) tetraisopropoxide, TTIP, modified with silane coupling agent, (MSMA) were investigated.

3.3.2.1 TiO_2 Powder Modified with Silane Coupling Agent, 3-(3-methoxysilyl) propylmethacrylate, (MSMA)

Thermal stability of TiO_2/SiO_2 nanoparticles prepared by modifiying TiO_2 powder with MSMA was very high. Pyrolysis analysis of the sample yielded a spectra involving only loss of side chains of silane coupling agent as shown in Figure 3.8 at around 424 °C. Products due to loss of CH_2CCH_3 (m/z=41), CO_2(m/z=44), CH_2CCH_3COO (m/z=69), and due to hydrolyzation of silane coupling agent such as O_2SiOH (m/z=77), O_2SiOCH_3 (m/z=91) were detected (Figure 3.9).

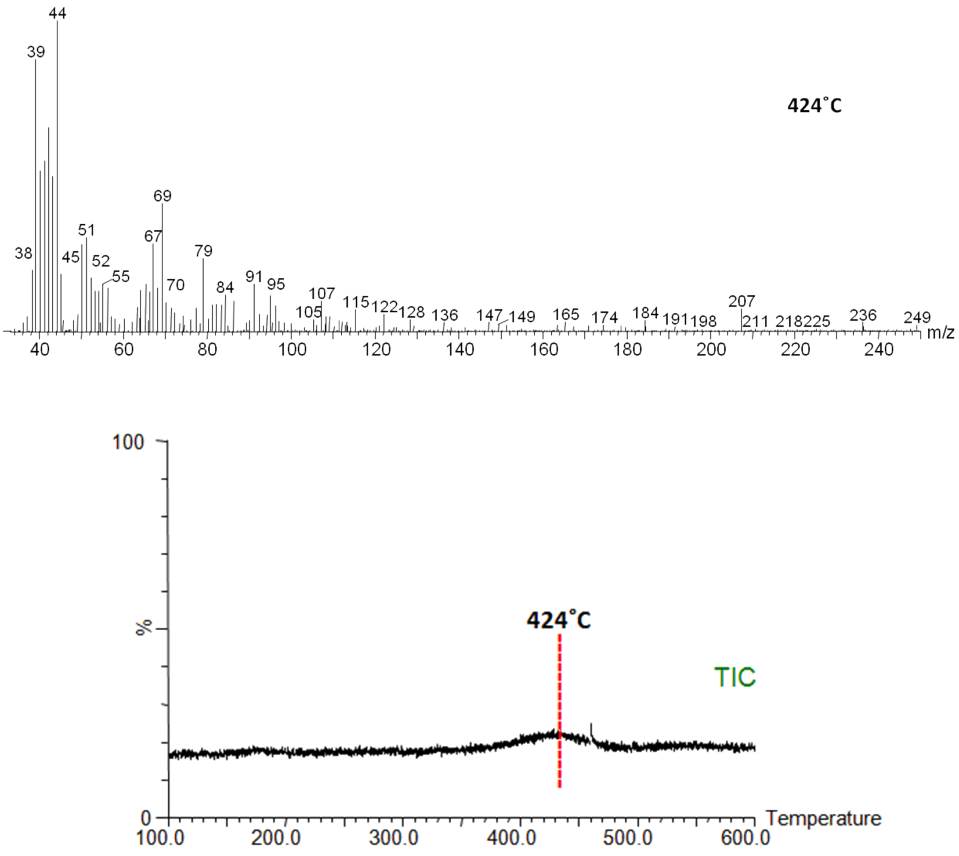

Figure 3.8: The TIC curve and the pyrolysis mass spectra recorded during the pyrolysis of exsitu TiO_2/SiO_2

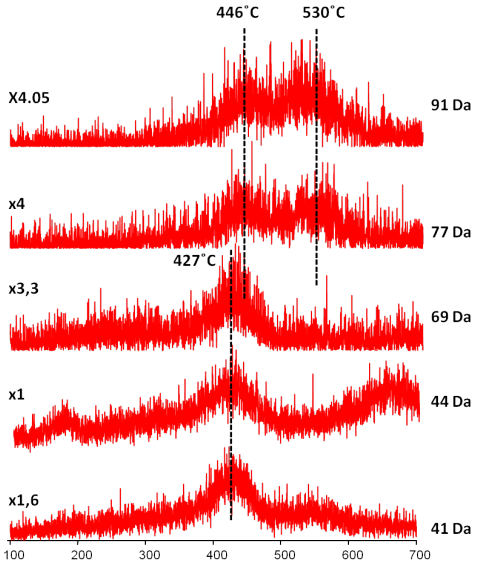

Figure 3.9: Single ion evolution profiles of some selected thermal decomposition products of exsitu TiO_2/SiO_2

3.3.2.2 Titanium(IV) Tetraisopropoxide modified with Silane Coupling Agent, 3-(3-methoxysilyl) propylmethacrylate, (MSMA)

The total ion current curve of titanium(IV) tetraisopropoxide modified with 3-(3-methoxysilyl) propylmetacrylate with two broad peaks and a high temperature shoulder is in accordance with the complex structure. The TIC curve and the pyrolysis mass spectra at the peak maxima at 305, 418 and 453 °C recorded during the pyrolysis of TiO_2/SiO_2 are shown in Figure 3.10.

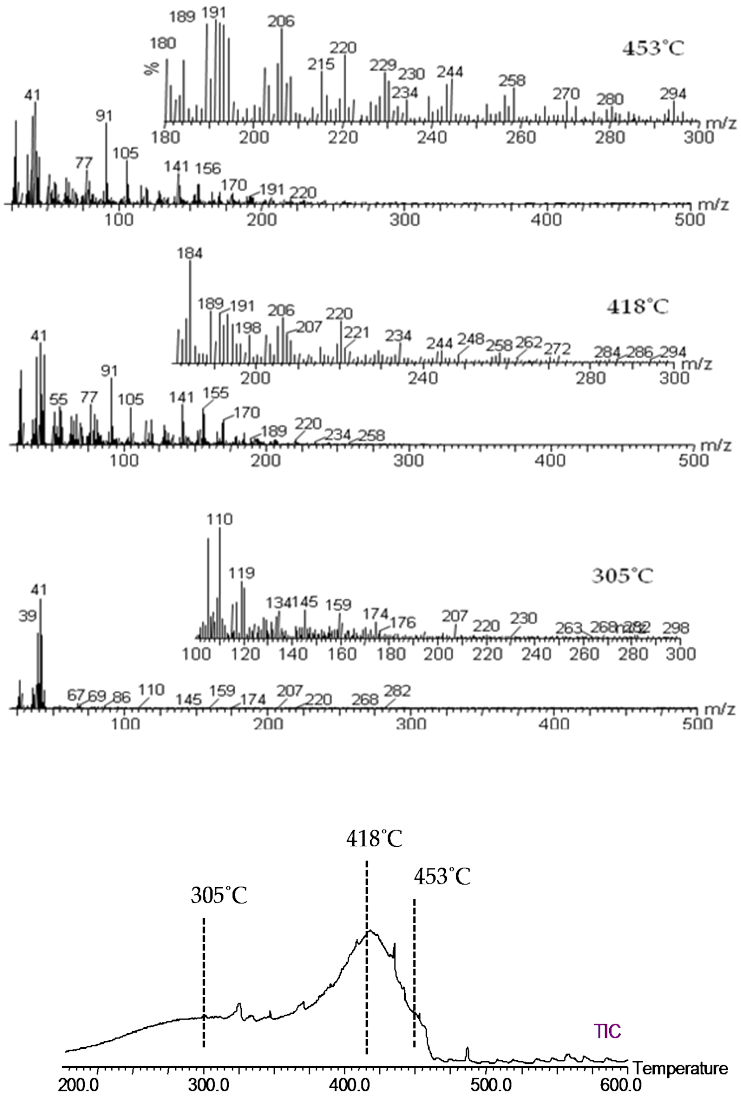

Figure 3.10: The TIC curve and the pyrolysis mass spectra recorded during the pyrolysis of TiO_2/SiO_2

The mass spectra recorded at around 305 °C were dominated with peaks due to $CH_2C(CH_3)$ (m/z=41 Da) indicating that thermal decomposition was started by loss of end groups. As the temperature increased, more complex spectra were recorded.

$Ti(OCH(CH_3)_2)_4$ was used as precursor of the titania particles. Hydrolyzation of these particles may yield several compounds with formula $Ti(OCH(CH_3)_2)_n(OH)_{4-n}$ where n=0 to 4. Presence of related peaks confirmed hydrolyzation of titania particles. Single ion evolution profiles of $Ti(OCH(CH_3)_2)_n(OH)_{4-n}$ based thermal decomposition products of TiO_2/SiO_2 for n=0 (m/z=116), n=1 (m/z=158), n=2 (m/z=200), n=3 (m/z=242) and n=4 (m/z=284) (Figure 3.11), showed that $Ti(OH)_4$ is the most abundant among all of them indicating that hydrolyzation occurred to a significant extent. Furthermore, in general, as the number of OH groups decreased thermal stability of the titania particles increased; $Ti(OCH(CH_3)_2)_3OH$ and $Ti(OCH(CH_3)_2)_4$ have the highest thermal stability, whereas $Ti(OCH(CH_3)_2)(OH)_3$ is the least stable one.

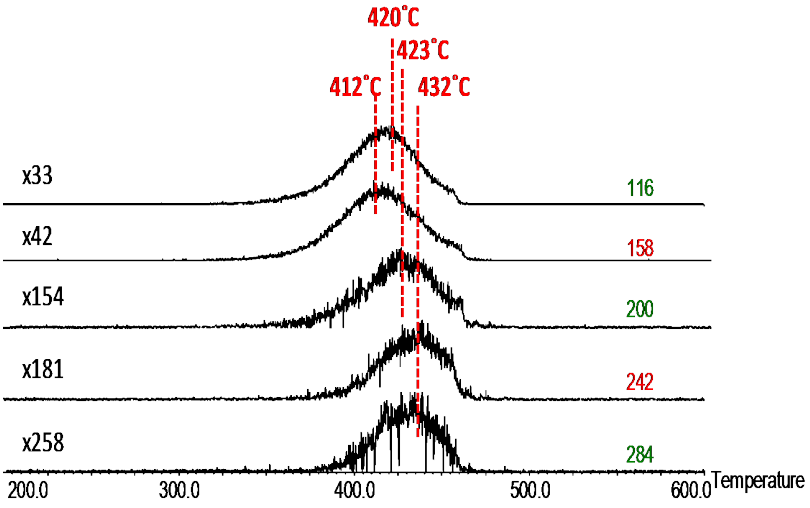

Figure 3.11: Single ion evolution profiles of -$Ti(OCH(CH_3))_n(OH)_{4-n}$ based thermal decomposition products of TiO_2/SiO_2 for n=0 (m/z=116), n=1 (m/z=158), n=2 (m/z=200), n=3 (m/z=242) and n=4 (m/z=242)

Hydrolyzation of silane coupling agent MSMA is also possible. Several diagnostic peaks indicating hydrolyzation of MSMA were detected. In Scheme 3.2., fragmentation pattern of silane coupling agent is shown. The intense and

characteristic peaks detected in the pyrolysis mass spectra of MSMA and the assignments made are given in Table 3.2.

Inspection of single ion evolution profiles of Si-$(OCH_3)_n(OH)_{3-n}$ based thermal decomposition products of TiO_2/SiO_2 showed that $Si(OH)_3$ is the most abundant among all the possible structures indicating that, most of the MSMA was hydrolyzed during the functionalization process as expected (Figure 3.12).

Scheme 3.2: Fragmentation pattern of silane coupling agent (MSMA)

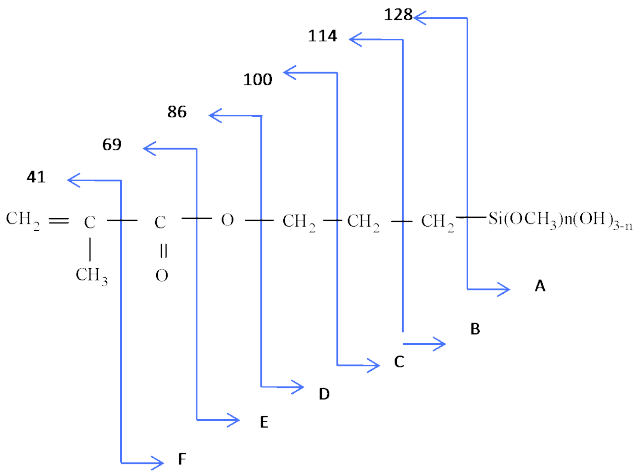

Table 3.2: The fragments detected for silane coupling agent (MSMA)

	n=0	**n=1**	**n=2**	**n=3**
A	79	93	107	121
B	93	107	121	135
C	107	121	135	149
D	121	135	149	163
E	137	151	165	179
F	165	179	193	207
Molecule	206	220	234	248

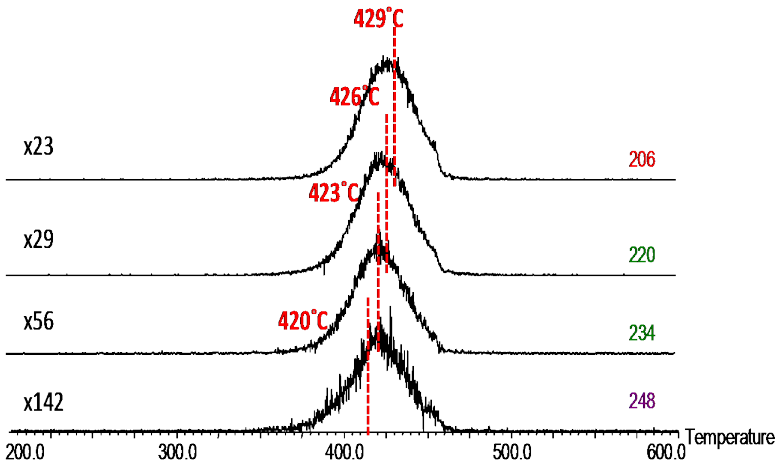

Figure 3.12: Single ion evolution profiles of Si-$(OCH_3)_n(OH)_{3-n}$ based thermal decomposition products of TiO_2/SiO_2 for n=0 (m/z=206), n=1 (m/z=220), n=2 (m/z=234) and n=3 (m/z=248)

Peaks indicating generation of CH_2CCH_3COOH (methacrylic acid) as shown in Scheme 3.3, and peaks pointing out its polymerization were also detected. Single ion evolution profiles of CH_2CCH_3COOH (methacrylic acid), monomer (m/z=86), dimer (m/z=172), trimer (m/z=258) are shown in Figure 3.13. Loss of methacrylic acid mainly took place at early stages of pyrolysis, at around 275 °C. On the other hand, evolution of dimer and trimer were detected above 400 °C. Existence of monomer peak in the pyrolysis mass spectra recorded in this region can directly be attributed to fragmentation of oligomers by dissociative ionization inside the MS.

Scheme 3.3: Generation of methacrylic acid

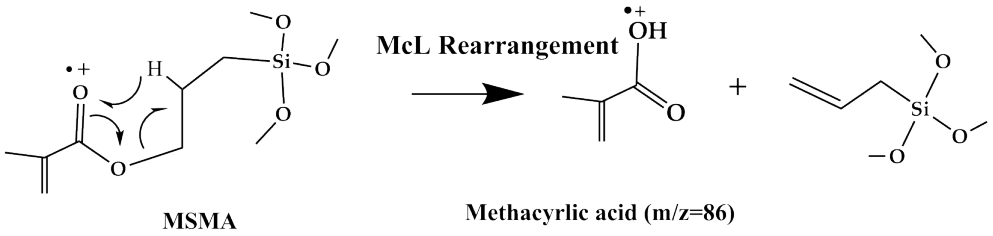

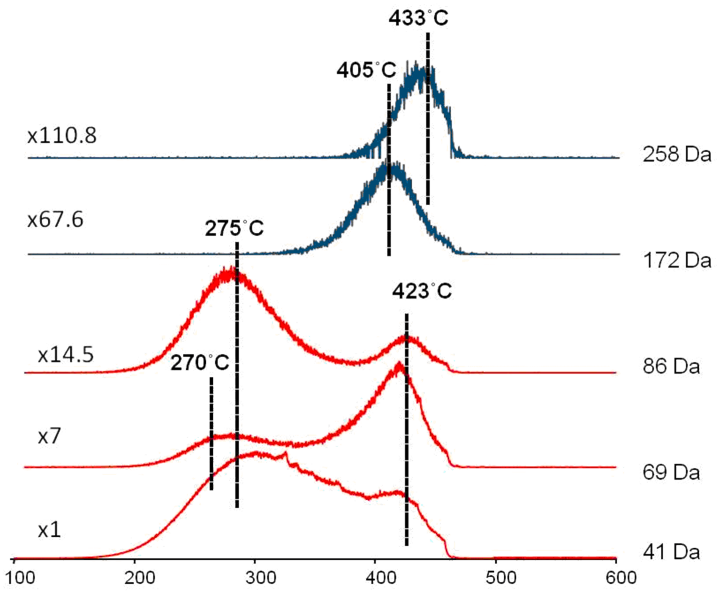

Figure 3.13: Single ion evolution profiles of CH_2CCH_3COOH (methacrylic acid) based thermal decomposition products of TiO_2/SiO_2, monomer (m/z=86), dimer (m/z=172), trimer (m/z=258)

During the synthesis, titania nanoparticles were coupled with silane coupling agent, (MSMA), to make titania compatible with the PMMA as mentioned earlier. Several possible reactions of titanium(IV)tetraisopropoxide (TTIP) and silane coupling agent (MSMA) yielding various structures are given in Scheme 3.4 and some possible pyrolysis and/or dissociative ionization products are shown in Scheme 3.5. The evolution profiles of some characteristic products involving Ti-O-Si linkages are given in Figure 3.14.

Scheme 3.4: Generation of Ti-O-Si linkages

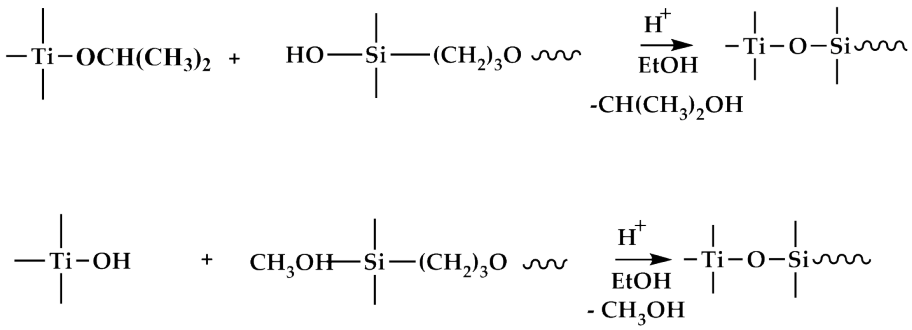

Scheme 3.5: Structures of ions generated from -Ti-O-Si- linkage

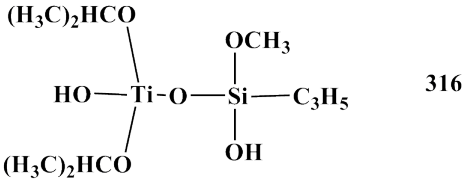

316

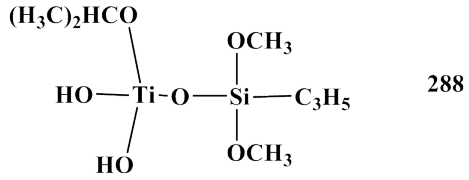

288

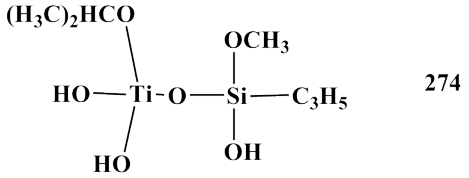

274

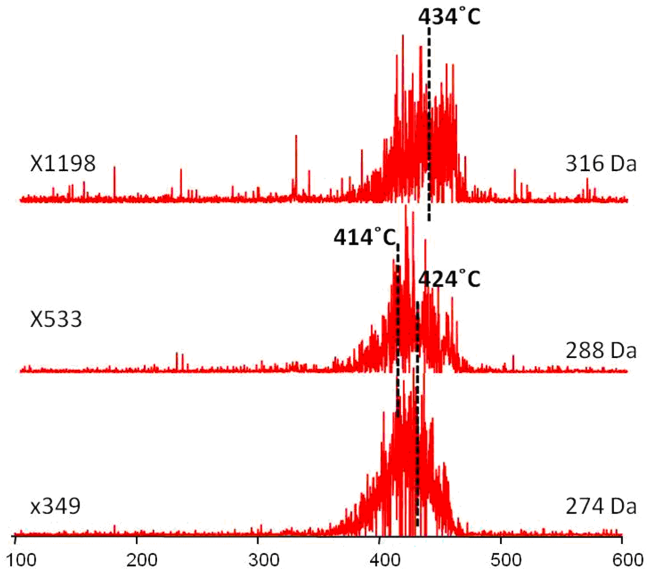

Figure 3.14: Single ion evolution profiles of -Ti-O-Si- linkage based thermal decomposition products of TiO_2/SiO_2

Formation of -Si-O-Si- and -Ti-O-Ti- linkages competes with the formation of -Ti-O-Si- linkages decreasing the amount of TiO_2/SiO_2 nanocomposite. -Si-O-Si- and -Ti-O-Ti- linkage formation reactions are shown in Scheme 3.6. a and b respectively. Single ion evolution profiles of some fragments involving -Si-O-Si- and -Ti-O-Ti- linkages are given in Figures 3.15 and 3.16 respectively.

Scheme 3.6: Generation of a) -Ti-O-Ti- and b) -Si-O-Si- linkages

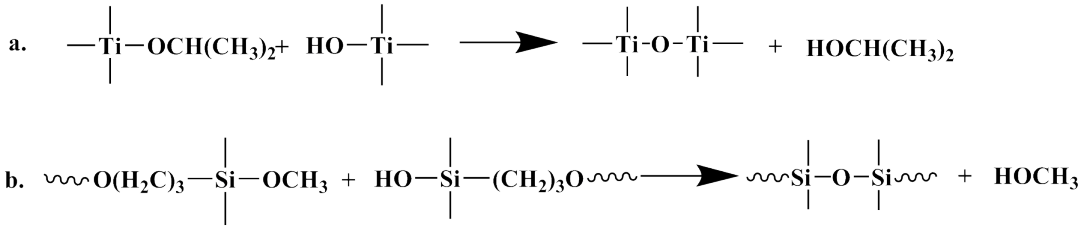

Molecular ion peaks for $Si_2O(OCH_3)_n(OH)_{4-n}(C_3H_6COOC(CH_3)CH_2)_2$ where n= 0 to 4, were not detected. Yet, fragments generated by loss of one or two methacrylic acid by McLafferty reactions, $Si_2O(OCH_3)_n(OH)_{4-n}(C_3H_5)(C_3H_6COOC(CH_3)CH_2)$ (m/z= 308, 322, 336, 350 and 364 for n=0 to 4 respectively) and $Si_2O(OCH_3)_n(OH)_{4-n}(C_3H_5)_2$ (m/z= 222, 236, 250, 264 and 278 for n=0 to 4 respectively) were detected. Among these fragments with n=0 are more abundant indicating that almost all OCH_3 groups were hydrolyzed in the acidic medium. In Figure 3.15., fragments $Si_2O(C_3H_6)_2$ (m/z=156), $Si_2O(OH)_4(C_3H_5)_2$ (m/z=222), $Si_2O(OH)_3(OCH_3)(C_3H_5)_2$ (m/z=236), $Si_2O(OH)_4(C_3H_5)C_3H_6CO_2C_3H_5$ (m/z=308) and $Si_2O(OH)_3(OCH_3)(C_3H_5)C_3H_6CO_2C_3H_5$ (m/z=322) are shown.

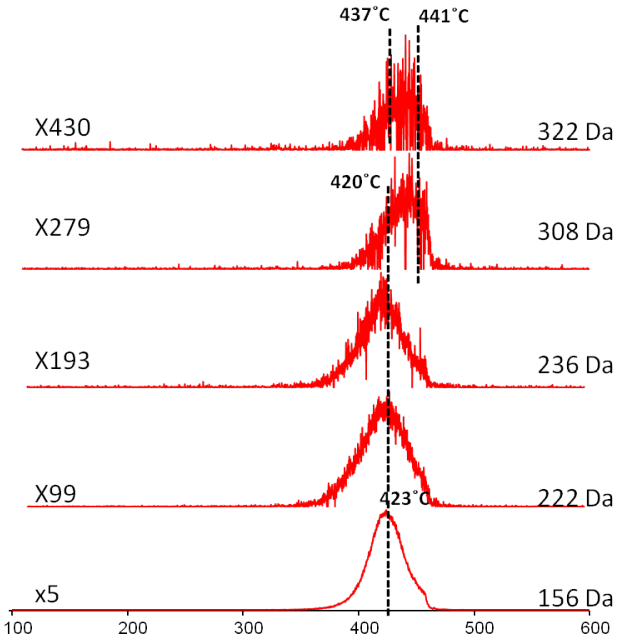

Figure 3.15: Single ion evolution profiles of Si-O-Si linkage based thermal decomposition products of TiO_2/SiO_2

Among $Ti_2O(OCH(CH_3)_2)_m(OH)_{6-m}$ where m= 0 to 6, products with m=5 and 6 were the less abundant indicating that hydrolyzation was quite efficient, more than 66%. The yield of these products were maximized in the temperature range 430 to 438 ° C. Single ion evolution profiles of -Ti-O-Ti- linkage based thermal decomposition products of TiO_2/SiO_2 namely, $Ti_2O(OH)_6$ (m/z=214), $Ti_2O(OCH(CH_3)_2)(OH)_5$ (m/z=256), $Ti_2O(OCH(CH_3)_2)_2$ $(OH)_4$ (m/z=298) are given in Figure 3.16.

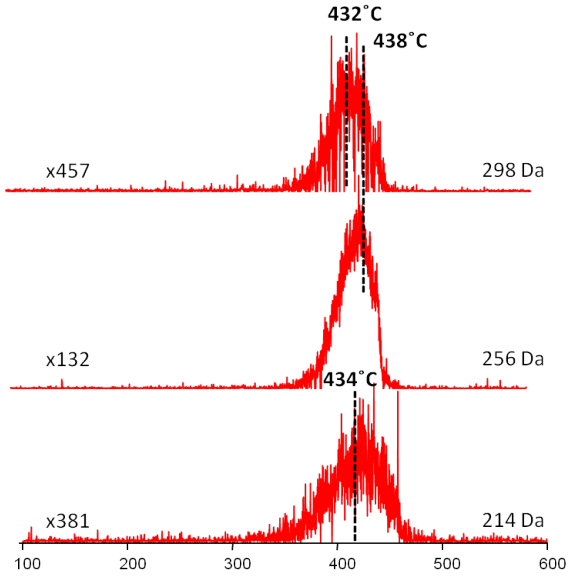

Figure 3.16: Single ion evolution profiles of -Ti-O-Ti- linkage based thermal decomposition products of TiO_2/SiO_2

During the pyrolysis process, polymerization of vinylene groups of silane coupling agent is also possible as shown in Scheme 3.7. Such reactions should yield fragments with different stabilities.

Scheme 3.7: Polymerization reaction of silane coupling agent

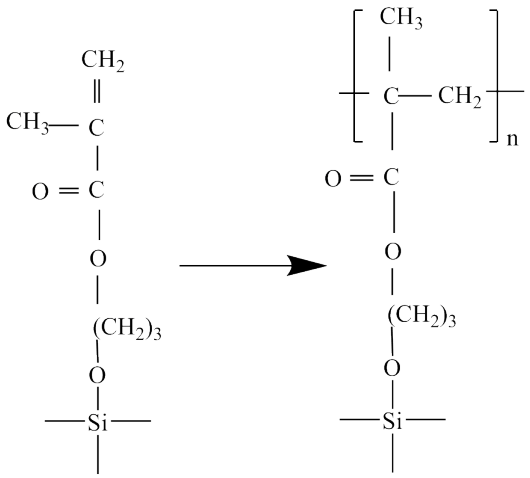

Single ion evolution profiles of some selected thermal decomposition products of TiO_2/SiO_2 namely, methacrylic acid (m/z=86), $Ti(OH)_4$ (m/z=116), $Si_2O(C_3H_6)_2$ (m/z=156), $(CH_2)_3OCOC(CH_2)CH_3Si(OCH_3)_3$ (m/z=206) and -Ti-O-Si- (m/z=274 in Scheme 3.5) are collected in Figure 3.17 to compare the thermal behavior of different products generated from Ti-O-Si, Si-O-Si, Ti-$(OCH(CH_3)_2)_n(OH)_{4-n}$, Si-$(OCH_3)_n(OH)_{3-n}$ or methacrylic acid during the pyrolysis. It is revealed from this figure that tendency of evolution of Si-O-Si linkages was more likely under the experimental conditions.

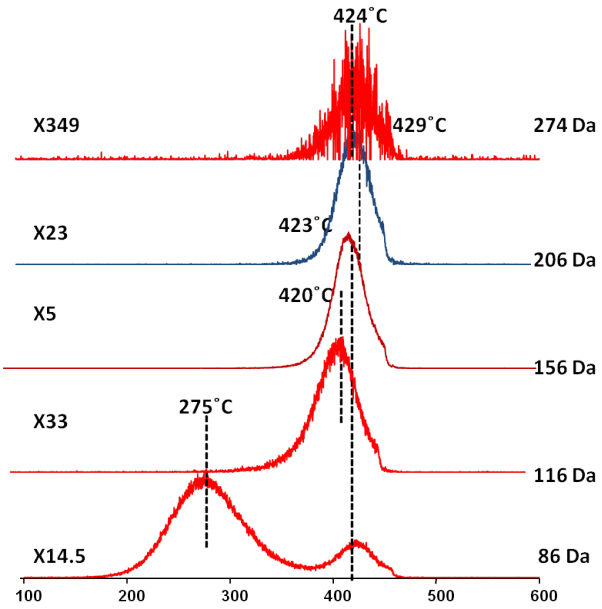

Figure 3.17: Single ion evolution profiles of some selected thermal decomposition products of TiO_2/SiO_2

In Table 3.3, the relative intensities and assignments made for intense and/or characteristic peaks recorded during the pyrolysis of TiO_2/SiO_2 prepared by modifying titanium(IV) tetraisopropoxide with silane coupling agent, 3-(3-methoxysilyl)propylmethacrylate, (MSMA) at 310 and 418 °C are collected.

Table 3.3: The relative intensities and assignments made for intense characteristic peaks for TiO_2/SiO_2

m/z	Relative Intensities		Assignments
	318 °C	418 °C	
41	1000	1000	C_3H_5.
69	33.4	222.9	CH_2CCH_3CO
77	3.6	389.8	O_2SiOH
82	8.8	308.0	$(CH_2CCH_3)_2$
86	43.5	35.6	CH_2CCH_3COOH
91	2.5	675.2	O_2SiOCH_3
115	1.5	246.1	$CH_2CH_2CCH_3CH_2COOCH_2CH_2$
116	0.3	44.9	$Ti(OH)_4$
119	1.7	233.4	$OSiOCH_3(OCH_2CH_2)$
128	0.8	191.5	$CHCH_3CH_2COOCH_2CH_2CH_2$
141	0.1	407.4	$CH_2CH_2CCH_3COOCH_2CH_2CH_2$,
142	0.3	230.4	$CH_2CCH_3COOCH_2CH_2CHO$, $CH_3CH_2CCH_3COOCH_2CH_2CH_2$
155	0.1	360.9	$(CCH_3CH_2COOH)CCH_3CH_2CO$,
156	0.0	314.8	$H(CCH_3CH_2COOH)CCH_3CH_2CO$
158	0.0	31.9	$Ti(OCH(CH_3)_2)(OH)_3$
165	0.1	126.5	$(HO)_3Si(CH_2)_3COO$
168	0.0	22.4	$(CH_2CCH_3)_2COO(CH_2)_3$
172	0.1	17.2	$(CH_2CCH_3COOH)_3$
179	0.0	83.8	$(CH_3O)_3Si(CH_2)_3O$
200	0.0	7.4	$Ti(OCH(CH_3)_2)_2(OH)_2$
206	0.0	60.5	$CH_2CCH_3CO_2(CH_2)_3Si(OH)_3$
214	0.0	3.5	$(OH)_3TiOTi(OH)_3$
220	0.0	49.0	$CH_2CCH_3COO(CH_2)_3Si(OCH_3)(OH)_2$
222	0.1	7.7	$Si_2O(OH)_4(C_3H_5)_2$
234	0.0	23.1	$CH_2CCH_3COO(CH_2)_3Si(OCH_3)_2(OH)$
236	0.0	4.0	$Si_2O(OH)_3(OCH_3)(C_3H_5)_2$
248	0.0	9.4	$CH_2CCH_3COO(CH_2)_3Si(OCH_3)_3$
256	0.0	3.6	$((CH_3)_2CHO)(OH)_2TiOTi(OH)_3$
258	0.0	11.6	$(CH_2CCH_3COOH)_3$
274	0.0	1.2	$(OH)_2(OCH(CH_3)_2)TiOSi(OH)(OCH_3)C_3H_5$
284	0.0	2.1	$Ti(OCH(CH_3)_2)_4$
288	0.0	0.6	$(OH)_2(OCH(CH_3)_2)TiOSi(OCH_3)_2C_3H_5$
298	0.0	0.8	$Ti_2O(OCH(CH_3)_2)_2(OH)_4$
308	0.0	0.7	$Si_2O(OH)_4(C_3H_5)C_3H_6COOC_3H_5$
316	0.0	0.2	$(OH)(OCH(CH_3)_2)_2TiOSi(OH)(OCH_3)C_3H_5$
322	0.0	0.8	$Si_2O(OH)_3(OCH_3)(C_3H_5)C_3H_6COOC_3H_5$

3.3.3 Insitu SiO_2/TiO_2/PMMA

TIC curves of 5%, 10%, 20% and 30% insitu TiO_2/SiO_2/PMMA are given in Figure 3.18. The TIC curve of pure PMMA is also included for comparison. The peak maximum in the TIC curves shifted from 438 to 411 °C as the TiO_2/SiO_2 percentage increased from 5% to 30% for insitu TiO_2/SiO_2/PMMA samples. For 10% and 20% insitu TiO_2/SiO_2/PMMA peak maximum was recorded at around 420 and 418 °C respectively, pointing out that as the weight percent of functionalized titania increased the thermal stability of PMMA decreased. Table 3.4 shows the relative intensities and the assignments made for the intense and/or characteristic peaks recorded in the pyrolysis mass spectra of 5%, 10%, 20% and 30% insitu TiO_2/SiO_2/PMMA. The data for TiO_2/SiO_2 was also included for comparison.

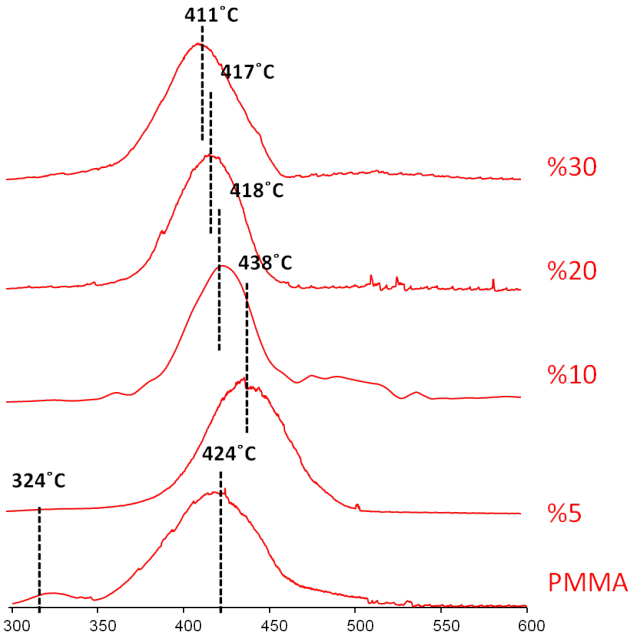

Figure 3.18: TIC curves of 5%, 10%, 20%, 30%, insitu TiO_2/SiO_2/PMMA

Analysis of pyrolysis mass spectra indicated that in general, as the weight percentage of TiO_2/SiO_2 increased relative yields of TiO_2/SiO_2 based products increased significantly. For investigation of the effect of amount of titania in PMMA on thermal stability of PMMA, pyrolysis mass spectrometric results of 5% and 20% insitu TiO_2/SiO_2/PMMA are discussed in details.

Table 3.4: The relative intensities and assignments made for intense and/or characteristic peaks for 5%, 10%, 20%, 30% insitu TiO_2/SiO_2/PMMA

m/z	Relative Intensities					Assignments
	TiO_2/SiO_2	5%	10%	20%	30%	
	420 °C	438 °C	420 °C	418 °C	411 °C	
41	1000	966	952	900	970	C_3H_5
69	223	1000	1000	1000	1000	CH_2CCH_3CO
77	390	9.3	10.9	16.5	19.5	O_2SiOH
82	308	42.4	51.7	104	227	$(CH_2CCH_3)_2$
86	35.6	6.5	7.5	14.1	22.2	CH_2CCH_3COOH
91	675	4.8	8.8	13.6	15.7	O_2SiOCH_3
100	8.2	158	210	468	744	MMA, $CH_2CCH_3COOCH_3$
109	12.7	5.4	8.1	13.9	18.3	$CCH_3(CH_2CCH_3)_2$
115	246	1.4	3.5	4.2	8.8	$CH_2CH_2CCH_3CH_2COOCH_2CH_2$
116	44.9	0.3	1.0	1.1	4.9	$Ti(OH)_4$
119	233	1.8	2.4	3.4	1.4	$OSiOCH_3(OCH_2CH_2)$
128	192	1.9	3.4	5.5	5.4	$CHCH_3CH_2COOCH_2CH_2CH_2$
141	407	2.5	4.6	6.6	8.8	$CH_2CH_2CCH_3COOCH_2CH_2CH_2$,
142	230	1.7	3.0	6.4	8.1	$CH_3CH_2CCH_3CO_2C_3H_6$
155	361	1.7	3.3	5.7	7.4	$(CCH_3CH_2COOH)CCH_3CH_2CO$,
156	315	0.8	1.8	2.7	3.5	$H(CCH_3CH_2COOH)CCH_3CH_2CO$
158	31.9	0.3	0.6	1.0	1.3	$Ti(OCH(CH_3)_2)(OH)_3$
165	127	1.2	2.3	3.7	5.0	$(HO)_3Si(CH_2)_3COO$
168	22.4	1.0	3.2	5.9	9.3	$(CH_2CCH_3)_2COO(CH_2)_3$
172	17.2	0.1	0.7	1.2	1.2	$(CH_2CCH_3COOH)_2$
179	83.8	0.5	0.2	2.4	3.4	$(CH_3O)_3Si(CH_2)_3O$
200	7.4	0.4	0.9	2.0	3.2	MMA dimer, $Ti(OCH(CH_3)_2)_2(OH)_2$
206	60.5	0.1	0.5	0.7	0.9	$CH_2CCH_3CO_2(CH_2)_3Si(OH)_3$
214	3.5	0.2	0.7	1.4	1.7	$(OH)_3TiOTi(OH)_3$
220	49.0	0.1	0.5	0.7	0.8	$CH_2CCH_3COO(CH_2)_3Si(OCH_3)(OH)_2$
222	14.2	0.1	0.6	0.8	1.1	$Si_2O(OH)_4(C_3H_5)_2$
234	23.1	0.1	0.3	0.6	1.0	$CH_2CCH_3COO(CH_2)_3Si(OCH_3)_2(OH)$
236	6.2	0.2	0.5	0.9	1.2	$Si_2O(OH)_3(OCH_3)(C_3H_5)_2$
248	9.4	0.1	0.4	0.5	0.7	$CH_2CCH_3COO(CH_2)_3Si(OCH_3)_3$
256	3.6	0.1	0.5	0.6	0.9	$((CH_3)_2CHO)(OH)_2TiOTi(OH)_3$
258	11.6	0.0	0.2	0.2	0.5	$(CH_2CCH_3COOH)_3$
271	3.6	0.1	0.4	0.7	0.9	$(HO)((CH_3)_2CHO)TiOSi(OCH_3)_2C_3H_5$
274	1.4	0.1	0.3	0.2	0.3	$(OH)_2(OCH(CH_3)_2)TiOSi(OH)(OCH_3)C_3H_5$
284	2.1	0.0	0.1	0.2	0.2	$Ti(OCH(CH_3)_2)_4$
288	0.4	0.0	0.3	0.2	0.5	$(OH)_2(OCH(CH_3)_2)TiOSi(OCH_3)_2C_3H_5$
300	1.6	0.4	0.7	0.8	1.9	MMA trimer
308	1.9	0.0	0.4	0.2	0.4	$Si_2O(OH)_4(C_3H_5)C_3H_6COOC_3H_5$
316	0.2	0.0	0.3	0.2	0.3	$(OH)(OCH(CH_3)_2)_2TiOSi(OH)(OCH_3)C_3H_5$
322	1.5	0.0	0.4	0.0	0.1	$Si_2O(OH)_3(OCH_3)(C_3H_5)C_3H_6COOC_3H_5$

3.3.3.1 5% insitu and 20% insitu TiO_2/SiO_2/PMMA

The total ion current curve recorded during the pyrolysis of 5% insitu TiO_2/SiO_2/PMMA is shown in Figure 3.19.

TIC curve of 5% insitu TiO_2/SiO_2/PMMA showed a peak maximum at around 439 °C. As can be seen in Figure 3.6., even the high temperature peak with a maximum at 424 °C in the TIC curve of pure PMMA is lower than that of the corresponding one for 5% insitu TiO_2/SiO_2/PMMA. The disappearance of low temperature peak present in the TIC curve of PMMA may be associated with removal of low molar mass PMMA chains during the functionalization process.

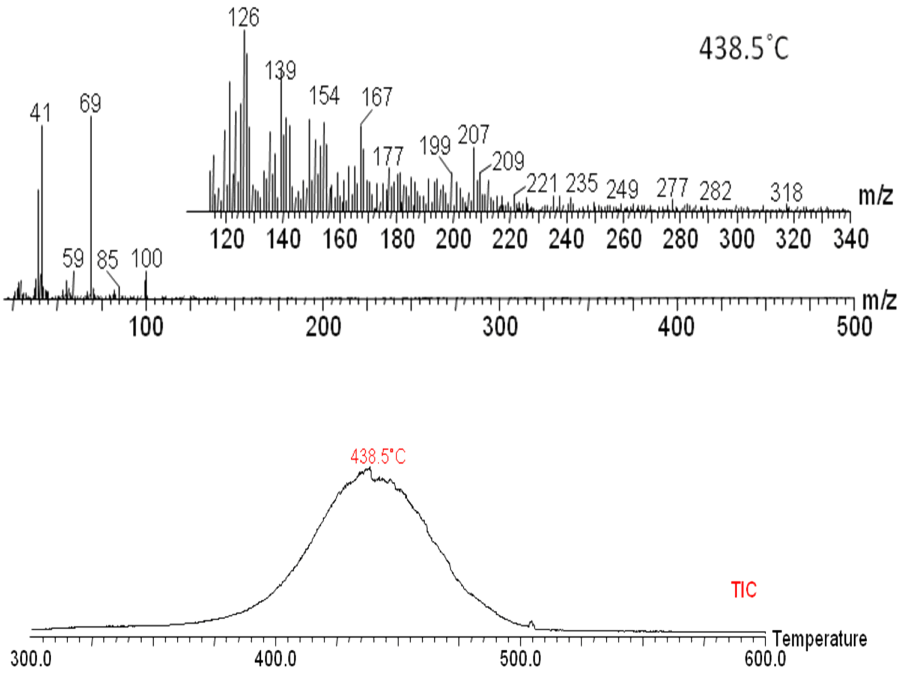

Figure 3.19: TIC curve and the pyrolysis mass spectra recorded during the pyrolysis of 5% insitu TiO_2/SiO_2/PMMA

To get a better idea, single ion evolution profiles of some selected thermal decomposition products of 5% insitu TiO_2/SiO_2/PMMA, namely CH_2CCH_3CO (m/z=69), $CH_2CCH_3COOCH_3$ (m/z=100), $(CH_2CCH_3COOCH_3)_3$ (m/z=300), CH_2CCH_3COOH (m/z=86), $(CH_2CCH_3COOH)_2$ (m/z=172) ,$CH_2CH_2CCH_3COOCH_2CH_2CH_2$ (m/z=141), $(CCH_3CH_2COOH)CCH_3CH_2CO$ (m/z=155), $(OH)_3TiOTi(OH)_3$ (m/z=214), $(HO)((CH_3)_2CHO)TiOSi(OCH_3)_2C_3H_5$

(m/z=271) are shown in Figure 3.20. It can be noted from the figure that products due to fragmentation of functionalized titania in PMMA reached maximum yield at 447° C, slightly higher than the corresponding value at 438 ° C for the PMMA based products.

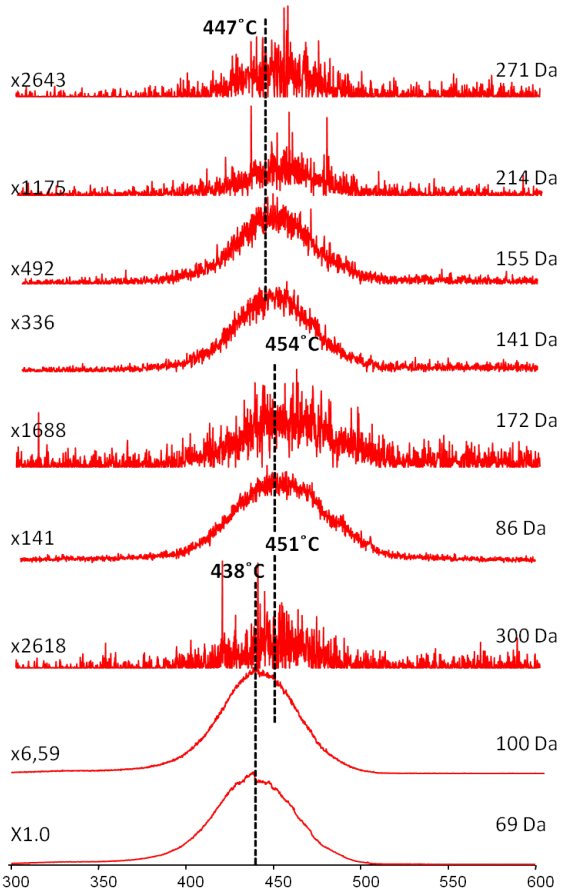

Figure 3.20: Single ion evolution profiles of some selected thermal decomposition products of 5% insitu TiO_2/SiO_2/PMMA

The total ion current (TIC) curve that is the variation of total ion yield as a function of temperature recorded during the pyrolysis of 20% insitu TiO_2/SiO_2/PMMA is shown in Figure 3.21. TIC cuve of 20% insitu TiO_2/SiO_2/PMMA showed a peak maximum at around 418 °C which is lower than the maximum of high temperature peak in the TIC curve of pure PMMA at 424 °C. Again the low temperature peak was disappeared.

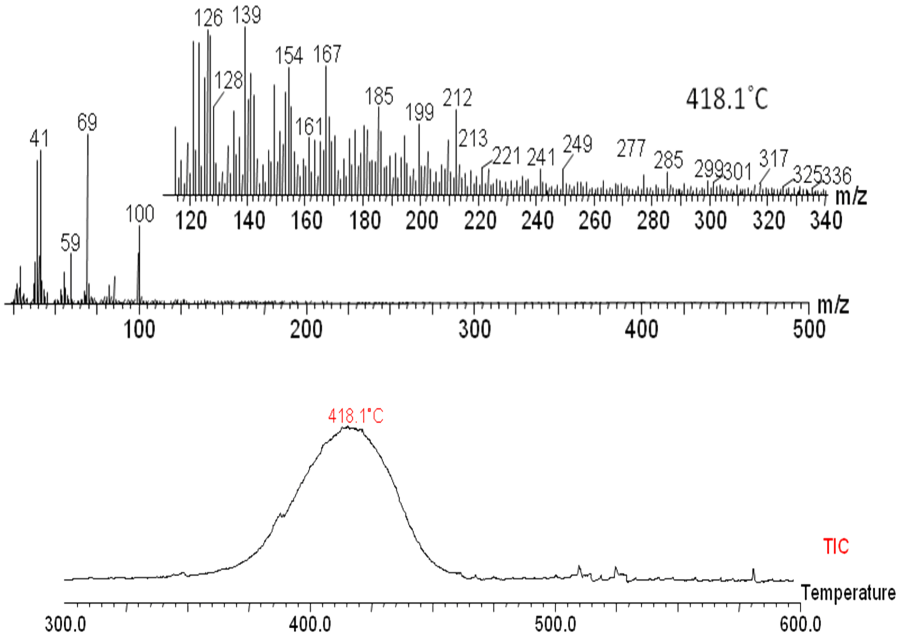

Figure 3.21: TIC curve and the pyrolysis mass spectra recorded during the pyrolysis of 20% insitu TiO_2/SiO_2/PMMA

Single ion evolution profiles of some selected thermal decomposition products of 20% insitu TiO_2/SiO_2/PMMA namely, CH_2CCH_3CO (m/z=69), $CH_2CCH_3COOCH_3$ (m/z=100), $(CH_2CCH_3COOCH_3)_3$ (m/z=300), CH_2CCH_3COOH (m/z=86), $(CH_2CCH_3COOH)_2$ (m/z=172) ,$CH_2CH_2CCH_3COOCH_2CH_2CH_2$ (m/z=141), (CCH_3CH_2COOH) CCH_3CH_2CO (m/z = 155), $(OH)_3TiOTi(OH)_3$ (m/z=214), $(HO)((CH_3)_2CHO)TiOSi(OCH_3)_2C_3H_5$ (m/z=271) were shown in Figure 3.22. Again the evolution profiles of functionalized titania products maximized at slightly higher temperatures, at around 424 ° C, than those of showing maximum when compared to pure PMMA based products showing maximum yield at around 418 ° C.

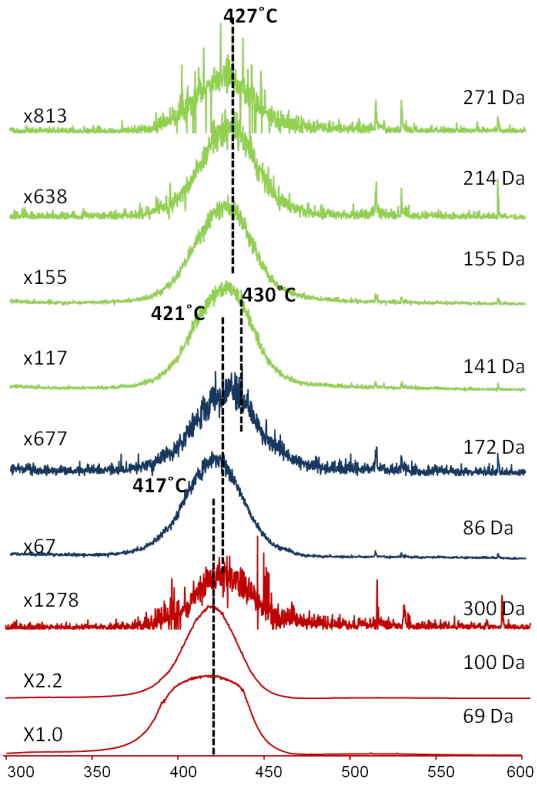

Figure 3.22: Single ion evolution profiles of some selected thermal decomposition products of 20% insitu TiO_2/SiO_2/PMMA

It is clear that as the weight percentage of TiO_2/SiO_2 increased the relative yields of TiO_2/SiO_2 based products increased as expected. Furthermore, increase in relative yields of MMA, its dimer and trimer were also noted indicating that thermal decomposition mechanism was changed in the presence of TiO_2/SiO_2 from depolymerization to random cleavages. During the incorporation of TiO_2/SiO_2, increasing the weight percent of TiO_2/SiO_2 in PMMA caused polymerization of silane coupling agents to form networks as shown in Scheme 3.7 yielding products such as $(CH_2CCH_3)_2$ (m/z=82). These polymerization reactions may be one of the reasons of loss of coupling agent (MSMA) and decrease in the compatibility of titania particles with the polymer matrix. However, the increase in the yield of CH_2CCH_3COOH acid with the increase in weight percentage of TiO_2/SiO_2 was even more significant. Thus, the decrease in thermal stability of PMMA with the increase in weight percentage of TiO_2/SiO_2 in PMMA may be due to the degradation of PMMA chains with the acid generated.

3.3.4 Exsitu TiO_2/SiO_2/PMMA

Direct pyrolysis mass spectrometry analyses of 5%, 10% and 20% exsitu TiO_2/SiO_2/PMMA were compared in Figure 3.23. The TIC curve of PMMA was also included for comparison. Table 3.4. shows the relative intensities and the assignments made for the intense and/or characteristic peaks recorded during the pyrolysis of 5%, 10%, 20% exsitu TiO_2/SiO_2/PMMA.

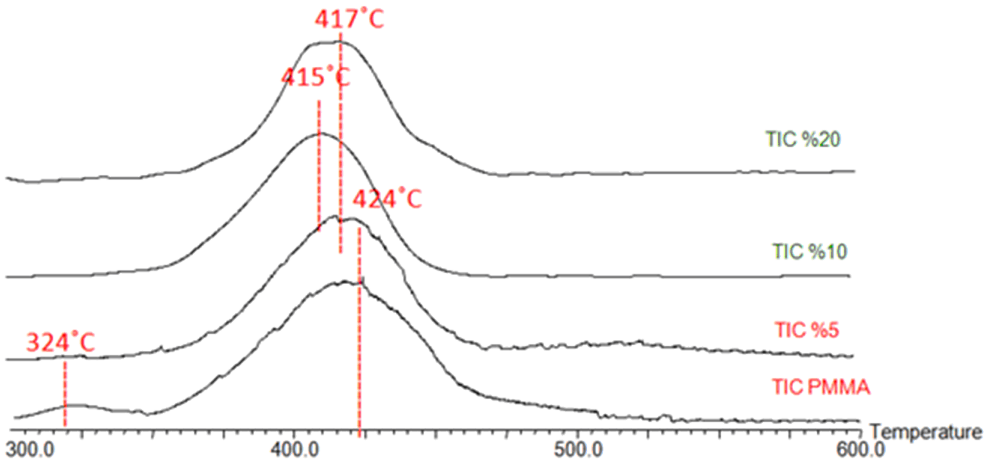

Figure 3.23: TIC curves of 5%, 10%, 20% exsitu TiO_2/SiO_2/PMMA

5%, 10%, 20% exsitu TiO_2/SiO_2/PMMA nanocomposites showed peak maxima at around 417°C, 415°C and 418°C respectively, slightly lower than PMMA. The total ion current (TIC) curves of 5%, 10% and 20% exsitu TiO_2/SiO_2/PMMA showed that thermal stability of PMMA decreased slightly in the presence of TiO_2 powder modified with silane coupling agent, 3-(3-methoxysilyl) propylmethacrylate, (MSMA) compared to pure PMMA, yet, the weight percentage of TiO_2/SiO_2 had no significant effect on thermal stability. Contrary to what was observed for insitu TiO_2/SiO_2/PMMA the yields of monomer, and low mass oligomers were decreased as the weight percentage of modified TiO_2 was increased. However, a decrease in the relative yields of silane based fragments was also noted as the weight percentage of modified TiO_2 was increased.

Table 3.5: The relative intensities and assignments made for intense characteristic peaks for 5%, 10%, 20% exsitu TiO_2/SiO_2/PMMA

m/z	Relative Intensities			Assignments
	5%	10%	20%	
	417 °C	**413.5 °C**	**417.9 °C**	
41	917	921	979	CH_2CCH_3
43	82	64	38	$CH(CH_3)_2$
59	314	274	160	$(CH_3)_2$ CHO
69	1000	1000	1000	$CH_2C(CH_3)O$
82	14.2	12.8	8.7	$(CH_2CCH_3)_2$
86	1.9	1.1	0.8	CH_2CCH_3COOH
100	558	423	182	M_{MMA}
127	9.4	8	4.4	$CH_2C(CH_3)COO(CH_2)_3$
154	8.5	7	3.3	$CH_2C(CH_3)COO(CH_2)_3Si$
217	1.8	1.1	0.9	$CH_2C(CH_3)COO(CH_2)_3Si(OCH_3)_2$
241	1.9	1.8	0.9	$Ti(OCH(CH_3)_2)_3O$
331	0.6	0.4	0.2	$Ti(OCH(CH_3)_2)_3OSiO(Me)_2$

As an example the total ion current (TIC) curve that is the variation of total ion yield as a function of temperature recorded during the pyrolysis of 20% exsitu TiO_2/SiO_2/PMMA is shown in Figure 3.24.

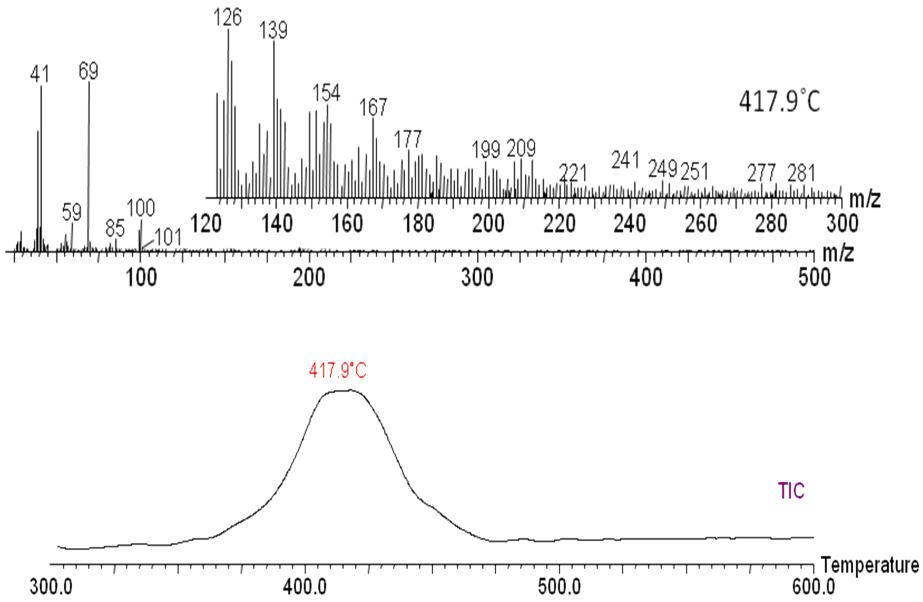

Figure 3.24: TIC curve and the pyrolysis mass spectra recorded during the pyrolysis of 20% exsitu TiO_2/SiO_2/PMMA

Single ion evolution profiles of intense and / or characteristic products namely CH_2CCH_3 (m/z=41), $CH(CH_3)_2$ (m/z=43), $(CH_3)_2CHO$ (m/z=59), $CH_2C(CH_3)O$ (m/z=69), $(CH_2CCH_3)_2$ (m/z=82), CH_2CCH_3COOH (m/z=86), M_{MMA} (m/z=100), $CH_2C(CH_3)COO(CH_2)_3$ (m/z = 127), $CH_2C(CH_3)COO(CH_2)_3$ Si (m/z=154), $CH_2C(CH_3)COO(CH_2)_3Si(OCH_3)_2$ (m/z=217), $Ti(OCH(CH_3)_2)3O$ (m/z=241), are shown in Figure 3.25. Inspection of single ion evolution profiles of intense and characteristic products indicated that acid generation shifted slightly to lower temperatures compared to insitu TiO_2/SiO_2 and followed almost a similar pathway with those of PMMA based products. This may be due to stronger interactions of silane groups with TiO_2, and loss of side chains during pyrolysis. The decrease in thermal stability may then be attributed to generation of methacrylic acid at lower temperatures as in case of 10, 20 and 30% insitu TiO_2/SiO_2/PMMA.

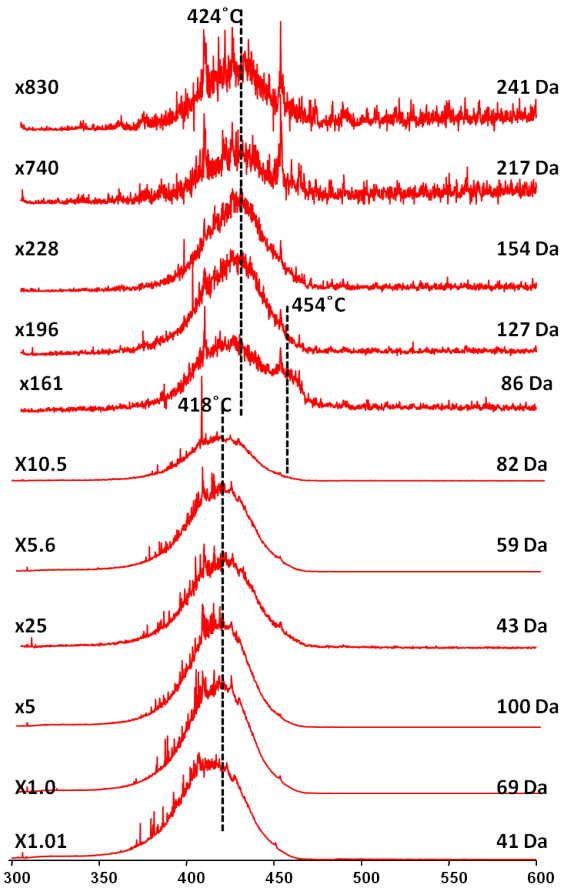

Figure 3.25: Single ion evolution profiles of some selected thermal decomposition products of 20% exsitu TiO_2/SiO_2/PMMA

CHAPTER 4

CONCLUSIONS

In this work, synthesis and characterization of nanostructural TiO_2/SiO_2 particles, insitu TiO_2/SiO_2/PMMA and exsitu TiO_2/SiO_2/PMMA nanocomposites have been aimed. The effect of incorporation of TiO_2/SiO_2 nanoparticles on thermal characteristics of PMMA was also investigated. TEM, ATR-FT-IR and Direct-Pyrolysis Mass spectroscopy techniques were applied for characterization.

Formation of nanostructural TiO_2/SiO_2 particles was confirmed by FT-IR and TEM. The results can be summarized as:

- ATR-FT-IR comfirmed TiO_2/SiO_2 network formation.
- TEM images showed the formation of TiO_2/SiO_2 and TiO_2/SiO_2/PMMA nanocomposites; the average particle size of SiO_2/TiO_2 nanoparticles was around 6 nm whereas average particle size of SiO_2/TiO_2/PMMA nanocomposites were around 25 nm. The increase in the size of nanoparticles is associated with incorporation of SiO_2/TiO_2 nanoparticles into PMMA matrix.
- Pyrolysis mass spectrometry pointed out
- Generation of Ti-O-Ti, Si-O-Si and Ti-O-Si linkages upon modification with silane coupling agent.
- Generation of methacrylic acid during the pyrolysis of insitu TiO_2/SiO_2.
- Increase in thermal stability of PMMA upon 5% (w/w) incorporation of insitu TiO_2/SiO_2 nanoparticles.

- Decrease in thermal stability of PMMA upon 10, 20 and 30% (w/w) incorporation of insitu TiO_2/SiO_2 nanoparticles due to evolution of methacrylic acid.
- Decrease in thermal stability upon incorporation of exsitu TiO_2/SiO_2 nanoparticles into PMMA.

It may be concluded that in case of insitu TiO_2/SiO_2 /PMMA, as the weight % of TiO_2/SiO_2 decreases, interactions between vinylene groups of silane coupling agent and PMMA increases; causing an increase in thermal stability. As the amount of acid generated decreases, thermal stability increases as a result of interactions of PMMA with silane groups. However, as the weight percentage of TiO_2/SiO_2 increased, opposing reactions became important and the amount of acid generated was also increased causing a decrease in thermal stability.

REFERENCES

[1] Davies, J. C., ***Woodrow Wilson International for Scholar***, April 2009, Oversight of Next Generation Nanotechnology

[2] Romero P. G., ”organic/inorganic Hybrid materials based on conducting organic polymers as electrodes for energy storage devices”, Thesis of Doctoral, Scientific researchers of the materials science institute of Barcelona, October 2003

[3] Dale W.S., Ryan S.J., ***American Chemical Society***, November 27 2007, ***40***, 8502-8519

[4] Zou, H., Wu, S., Shen, J., ***Chem. Rev.*** , 2008, ***108***, 3893-3957

[5] Mark, J. E., ***Acc. Chem. Res.*** , 2006, ***39***, 881-888

[6] Chen W.C., Lee SJ, Lee L.H., Lin J.L., ***J Mater Chem.***, 1999, ***9***, 2999

[7] Lee L.H., Chen W.C., ***Chem. Mater.***, 2001, ***13***, 1137

[8] Zhang J., Luo S.C., Gui L.L., ***J. Mater. Sci.***, 1997, ***32***, 1469

[9] Chang T.C., Wang Y.T., Hong Y.S., Chiu Y.S., ***Thermochim Acta.***, 2002, ***390***, 93

[10] Honma, I., Nomura, S., Nakajima H., ***J. Membr. Sci.***, 2001, ***185***, 83

[11] Paul D. R., Robeson L. M., ***Polymer***, April 2008, ***49***, 3187-3204

[12] Erdem, N., Cireli, A. A., Erdogan, U. H., ***J. Appl. Polym. Sci.***, 2009, ***111***, 2085-2091

[13] Yang, F., Nelson, G. L.,***Polym. AdV. Technol.***, 2006, ***17***, 320.

[14] Katsikis, N., Zahradnik, F., Helmschrott, A., Munstedt, H., Vital, A., ***Polym. Degrad. Stab***. 2007, ***92***, 1966

[15] Chatterjee A., ***J. Appl. Polym. Sci.***, 2010, ***116***, 3396-3407

[16] Rong Y., Chen H., Wu G., Wang M., ***Mat. Chem.***, November 2004, ***91***, 370-374

[17] Hsiue, G. H., Kuo, W. J., Huang, Y. P., Jeng, R., ***J. Polymer***, 2000, ***41***, 2813

[18] http://en.wikipedia.org/wiki/Sol-gel last accesed date: 20 July 2011

[19] Choi, H., ”Novel Preparation of Nanostructured Titanium Dioxide Photocatalytic Particles, Films, Membranes, and Devices for Environmental Applications”, Doctora of Philosophy Thesis, University of Cincinnati, Department of Civil and Environmental Engineering, 2006

[20] Liu, Y. L., Wu, C. S., Chiu, Y. S., Ho, W. H., ***J. Polym. Sci. Part A: Polym. Chem.*** , 2003, ***41***, 2354

[21] Honma, I., Hirakawa, S., Yamada, K., Bae, J., ***M. Solid State Ionics***, 1999, ***118***, 29

[22] Chang, H. Y., Lin, C. W., ***J. Membr. Sci.***, 2003, ***218***, 295

[23] Chang, H. Y., Thangamuthu R., Lin, C. W., ***J. Membr. Sci.***, 2004, ***228***, 217

[24] Wu, C. M., Xu, T. W., Yang, W. H., ***Eur. Polym. J.***, 2005, ***41***, 1901

[25] Zhang, S. L., Xu, T. W., Wu, C. M., ***J. Membr. Sci.***, 2006, ***269***, 142

[26] Saito, R., Kuwano, K., Tobe, T., ***J. Macromol. Sci.***, 2002, ***A39***, 171

[27] Saito, R., Mori, Y., ***J. Pure Appl. Chem.***, 2002, ***A39***, 915

[28] Mori, Y., Saito, R., ***J. Macromol. Sci., Pure Appl. Chem.***, 2003, ***A40***, 671

[29] Shen, L., Zhong, W., Wang, H. T., Du, Q. G., Yang, Y. L., ***J. Appl. Polym. Sci.***, 2004, ***93***, 2289

[30] Yuwono A.H., Xue J., Wang J., Elim H. I., Ji W., Li Y., ***J.Mat. Chem.***, 2003, ***13***, 1475-1479

[31] Zheng J., Zhu R., He., Cheng G., Wang H., Yao K., ***J. Appl. Pol. Sci.***, 2010, ***115***, 1975-1981

[32] Wang, H., Zhong, N., Du, Q., Yang, Y., Okamoto, H., Inoune, S., ***Polym. Bull.***, 2003, ***51***, 63-68

[33] Lin, M., Wang, H., Meng, S., Zhong, W., Li, Z., Cai, R., Chen, Z., Zhou, X., Du, Q., ***J. Pharm. Sci.***, 2007, ***96***, 1518-1526

[34] http://pecongress.org.pk/images/upload/books/Paper676.pdf, last accessed date: 13 August 2011

[35] Novak, B. M., ***AdV. Mater.***, 1993, ***5***, 422

[36] Sanchez, C., Ribot, R., ***New. J. Chem.***, 1994, ***18***, 1007

[37] Mammeri, F., Le Bourhis, E., Rozes, L., Sanchez, C., ***J. Mater. Chem.***, 2005, ***15***, 3787

[38] Schubert, U., Husing, N., Lorenz, A., ***Chem. Mater.***, 1995, ***7***, 2010

[39] Judeinstein, P., Sanchez, C., ***J. Mater. Chem.***, 1996, ***6***, 511

[40] Wen, J. Y., Wilkes, G. L., ***Chem. Mater.***, 1996, ***8***, 1667

[41] Schottner, G., ***Chem. Mater.***, 2001, ***13***, 3422

[42] Huang, H. H., Orler, B., Wilkes, G. L., ***Polym. Bull.***, 1985, ***14***, 557

[43] Schmidt, H., ***J. Non-Cryst. Solids***, 1985, ***73***, 681

[44] Chen, Y., Iroh, J. O., ***Chem. Mater.***, 1999, ***11***, 1218

[45] Pomogailo, A. D., ***Russ. Chem. ReV.***, 2000, ***69***, 53

[46] Kang, S., Hong, S. I., Choe, C. R., Park, M., Rim, S., Kim, ***J. Polymer***, 2001, ***42***, 879

[47] Sugimoto, H., Daimatsu, K., Nakanishi, E., Ogasawara, Y., Yasumura, T., Inomata, K., ***Polymer***, 2006, ***47***, 3754

[48] Liu, Y. L., Hsu, C. Y., Wang, M. L., Chen, H. S., ***Nanotechnology***, 2003, ***14***, 813

[49] Liu, Y. L., Hsu, C. Y., Hsu, K. Y., ***Polymer***, 2005, ***46***, 1851

[50] Su, Y. H., Wei, T. Y., Hsu, C. H., Liu, Y. L., Sun, Y. M., Lai, ***J. Y. Desalination***, 2006, ***200***, 656

[51] Liu, Y.L., Hsu, C. Y., Su, Y. H., Lai, J. Y., ***Biomacromolecules***, 2005, ***6***, 368

[52] Blum, F. D., ***Encyclopedia of Polymer Science and Technology***, Kroschwitz, J. I., Ed., John Wiley & Sons: Hoboken, NJ, 2004, ***8***, 38-50

[53] Yoshinaga, K., Shimada, J., Nishida, H., Komatsu, M., ***J. Colloid Interface Sci.***, 1999, ***214***, 180

[54] Yoshinaga, K., Tani, Y., Tanaka,Y., ***Colloid Polym. Sci.***, 2002, ***280***, 85

[55] Chang, C., Cheng, L., Huang, F., Lin, C., Hsieh, C., Wang, W., ***J. Sol-Gel. Sci. Technol.***, 2010, ***55***, 199-206

[56] Viratyaporn W., Lehman R. L., ***J. Therm. Anal. Calorim.***, 2011, ***103***, 267-273

[57] Laachachi, M., Cochez, M., Ferriol, J.M., Leroy, E. ***Mater. Lett.***, 2005, ***59***, 36

[58] Laachachi, Leroy E., Cochez M., Ferriol M., Lopez-Cuesta J.M, ***Polym. Degrad. Stab.***, 2005, ***89***, 344

[59] Caris C.H.M., van Elven L.P.M., van Herk A.M., German A.L., ***Br. Polym. J.***, 1989, ***21***, 133

[60] Sidorenko A., Minko S., Gafijchuk G., Voronov S., ***Macromolecules***, 1999, ***32***, 4539

[61] Erdem B., Sudol E.D., Dimonie V.L., El-Aasser M.S., ***J. Polym. Sci. Part A: Polym. Chem.***, 2000, ***38***, 4419

[62] Yang M., Dan Y., ***Colloid Polym. Sci.***, 2005, ***284***, 243

[63] Zhang C., Li Q., Li J., ***Synthetic Metals***, 7 June 2010, ***160***, 1699-1703

[64] Koziej D., Fischer F., Kranzlin N., ***American Chemical Society***, 2009, ***1***, 1097 1104

[65] Dzunuzovic, E., Marinovic-Cincovic, M., Vukovic, J., Jeremic, K., Nedeljkovic, J. M., ***Polym. Comp.***, 2009, ***30***, 737-742

[66] Kumutha, K., Alias, Y., ***Spect. Acta Part A***, 2006, ***64***, 442-447

[67] Hacaloglu J., Athar I., Toppare L., Yagci Y., ***J. Mac. Sci.***, 2003, ***40***, 605-615

[68] Webster O. W., Hertler W. R., Sogah D. Y., ***Am. Chem. Soc.***, 1983, ***105***, 5706

[69] Brockhaus V. A., Jenckel E., ***Macromol. Chem.***, 1956, ***12***, 263